International Journal of Applied Pharmaceutics

ISSN- 0975-7058 Vol 17, Issue 4, 2025

Original Article

IN-SILICO MOLECULAR DOCKING STUDIES, SYNTHESIS AND PRELIMINARY PHARMACOLOGICAL EVALUATION OF NEW PYRAZOLINE DERIVATIVES BEARING PYRIDINE RING SCAFFOLDS

MOHAMMED CHASIB MAWLA*[1], TAGREED N-A OMAR[2]

[1]Ministry of Health, Baghdad, Iraq. [2]Department of Pharmaceutical Chemistry, College of Pharmacy, University of Baghdad, Baghdad, Iraq
*Corresponding author: Mohammed Chasib Mawla; *Email: mohammed.mawla2200m@copharm.uobaghdad.edu.iq

Received: 01 Apr 2025, Revised and Accepted: 19 May 2025

ABSTRACT

Objective: The primary objective was to study biological activity *in vivo*, anti-inflammatory activity, antibacterial and antifungal activities, the synthesis of new pyrazoline derivatives 5(a-f) through derivatives bearing heterocyclic scaffolds, molecular docking studies, and the prediction of pharmacokinetic properties of potent molecules by the computational method.

Methods: The synthesis of new pyrazoline derivatives 5(a-f) through derivatives bearing heterocyclic scaffolds, characterized via melting point, TLC, and spectral data acquisition (ATR-FTIR-IR, NMR, and mass spectroscopy), and evaluated for *in vivo* using a rat paw edema model, anti-inflammatory activity with Diclofenac sodium as the standard and *in vitro* antimicrobial activity against g-positive**:** *Staphylococcus. aureus (S. aureu), Streptococcus. Pyogenes (S. Pyogenes)* and g-negative *Escherichia. coli (E. coli), Pseudomonas. Aeruginosa (P. aeruginosa)*and *Candida albicans* using the agar-well diffusion method, with amoxicillin and ciprofloxacin as the standard. and ADME for 5(a-f) were evaluated using Ligand Designer from Glide (SchrodingerLLC).

Results: The final compound protein of docking (5e and 5d) has the highest docking score (-8.009 and-7.937) in the case of estimating their anti-inflammatory activity, important amino acids in the COX2 enzyme. The final compounds 5a and 5f demonstrated considerable activity from 2 to 5 h. The anti-inflammatory efficacy of the final product was estimated *in vivo* using a rat paw edema model. They are all important in terms of antibacterial activity. The compounds with the highest docking scores-6.111,-5.964,-5.847,-5.841,-5.272 and-5.093) are 5e,5c,5b,5f,5a and 5d. When compared to DMSO (solvent and control), We used the well diffusion technique to determine the zone of inhibition for the six meticulously synthesized final compounds, then thoroughly tested the new hybrid derivatives for their antimicrobial efficacy against both g-positive and g-negative bacteria. The following fascinating results were obtained: As antimicrobial activity, the high activity all six compounds showed high activity by *Staphylococcus. aureus (S. aureu), Streptococcus. Pyogenes (S. Pyogenes)*: (5b, 5e,5c and 5f);), the high activity all six compounds given by *Escherichia. coli (E. coli), Pseudomonas. Aeruginosa (P. aeruginosa)* (5a, 5d, 5b, 5c and 5f); give high activity; the others ranging (moderate-inactive). Antifungal activity against *Candida albicans*, when compared with the drug fluconazole, (5a, 5b, 5c and 5f); the other final compounds were (moderate-inactive). The compounds.

Conclusion: The compounds were effectively synthesized, and the findings of the study on their biological efficacy show that the finished compounds contain drug-like properties.

Keywords: Pyrazoline derivatives, Chalcones, Pharmacological activity, ADME, Molecular docking

DOI: https://dx.doi.org/10.22159/ijap.2025v17i4.54404 Journal homepage: https://innovareacademics.in/journals/index.php/ijap

INTRODUCTION

Chalcone (1,3-diphenyl-2-propen-1-one), defined by the general formula (Ar-C=O-CH=CH-Ar), is a polyphenolic compound belonging to the flavonoid family as seen in "fig. 1"[1, 2].

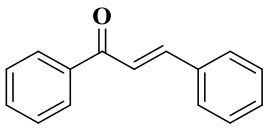

Fig. 1: Structure of chalcone

1,3-diphenyl-2-propen-1-ones are both naturally occurring and synthetically manufactured compounds, regarded as important intermediates in advanced chemical research due to their many replaceable hydrogens, which enable the production of diverse derivatives such as pyrazole. They are regarded as the basis for the synthesis of several compounds, including pyrazoline and pyrimidine [3]. Chalcones have a variety of pharmacological effects, encompassing antibacterial and anti-inflammatory activities [4]. Pyrazoline and its derivatives have significant biological activity and are classified as neutrophil chemicals [5, 6]; hence, they are essential in several pharmacological functions, including anti-inflammatory [7] and antimicrobial actions [8]. Dihydropyrazole is a five-membered heterocyclic compound whose stability is affected by the proximity of two nitrogen atoms and the endo-cyclic double bond, which varies in position among the three isomers of pyrazoline (1-pyrazoline, 2-pyrazoline, and 3-pyrazoline), with 2-pyrazoline being the most stable isomer fig. 2 [9]

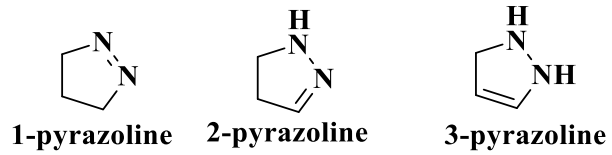

Fig. 2: Isomers pyrazoline

Pyrazoline derivatives exhibit increased biological activity and potential therapeutic applications, and combining them with substances such as sesamol, eugenol, and vanillin represents a significant advancement in medicinal chemistry. This combination aims to enhance the effectiveness of treating various illnesses, including cancer and inflammatory conditions, by leveraging the unique properties of each component. Numerous studies have demonstrated that pyrazoline derivatives possess strong anti-

inflammatory effects [10]. Incorporating the anti-inflammatory properties of natural compounds like vanillin and eugenol into pyrazoline derivatives may further enhance their therapeutic efficacy. This combination could broaden the pharmacological profile of pyrazolines, which already includes antimicrobial and antioxidant activities [11]. Consequently, this might facilitate the development of multi-target drugs that engage multiple pathways in disease processes. While the combination of these compounds holds promise, it is crucial to consider potential challenges, such as the requirement for extensive testing to ensure safety and efficacy in clinical applications. Sesamol, eugenol, and vanillin will be advantageous in the formulation and development of novel pharmaceuticals due to their capacity to inhibit superoxide anion production, mitigate hydroxyl radical generation, and function as effective free radical scavengers [12-14], in addition to possessing antibacterial properties. This work aimed to manufacture 2-pyrazoline derivatives conjugated with the antioxidants Sesamol, eugenol, and vanillin to enhance their antibacterial and anti-inflammatory properties. Our work employs computational methodologies such as ADME (absorption, distribution, metabolism, and excretion) and Molecular Docking is a technique used to predict the interactions between the ligand or drug and target proteins and the results of interaction are interpreted in terms of binding affinity, which is called the Docking score [15] molecular docking studies to aid in the search for new lead medications. Molecular docking is used in molecular modeling to predict the optimal binding orientation of two molecules to form a stable complex, and it is also essential to the rational creation of medications. The "best-fit" orientation of a ligand that binds to a certain target protein can be expressed in molecular docking, an optimization issue. In most cases, it reveals disease-causing proteins and aids in the discovery of novel medications [12, 16, 17].

MATERIALS AND METHODS

Hydrine hydrate (99%) was procured from Thomas Baker, while 2-acetylpyridine and methyl 2-chloroacetate were sourced from Shanghai Macklin Biochemical Company. Additional solvents and reagents were obtained from the chemical repository of the College of Pharmacy at the University of Baghdad. The reactions were meticulously analyzed utilizing Thin Layer Chromatography (TLC) with two distinct mobile solvent systems: A (chloroform: methanol, 85:15) and B (chloroform: ethylacetate: ether, 10:5:1). Melting points were ascertained employing a Stuart SMP30 electronic melting point apparatus. ATR-FTIR analysis was executed through the thin film methodology on a Shimadzu apparatus, and NMR spectra were recorded on a BRUKER Ultrashield. A molecular docking investigation was conducted at the College of Pharmacy, University of Baghdad, utilizing Schrodinger software.

Designing in silico

In silico test

The docking technique was started by acquiring the crystal structures of Diclofenac, the 3nl1 protein, and the penicillin-binding protein 3 from Mycobacterium tuberculosis (6KGV) from the Protein Data Bank. Subsequently, the Schrödinger-2023-Maestro laboratory executed a comprehensive methodology for protein synthesis. The main goal of this phase was the molecular extraction of free water from the location. Specific alterations were necessary to mitigate the danger of hydrogen bond overlap, so as to ensure a realistic depiction of the binding environment. Optimization efforts mostly focused on enhancing the protein's structure before docking. The ligands were manufactured with precision, akin to protein manufacturing. The objective of desalting these ligands was to eliminate impurities and improve the accuracy of their molecular structures [18, 19]. To enhance the ligands' participation in all possible chemical processes within the physiological pH range, we further synthesized all the tautomers. The comprehensive analysis of ligand-protein docking interactions stems from the precise ligand synthesis process. The receptor grid was established with FLP as the reference ligand following the production of the protein and ligand. The reference ligand was employed to generate the receptor grid in the binding pocket. By creating cubic boxes with dimensions of 25 Å for COX-2 and 30 Å for PBP3, the reference ligands will be included in the spatial parameters of subsequent docking simulations. The docking algorithm thoroughly examined all potential binding sites inside the confined space of the binding pocket, due to the precise construction of the grid. The primary objective was to employ Glide docking technology for adaptable sampling through conventional precision docking. This method enhanced the examination of diverse ligand orientations and conformations inside the receptor binding region, hence aiding the investigation of possible binding interactions. A dependable docking technique was developed by flexible sampling to clarify the complex interactions between ligands and COX-2 proteins. This systematic methodology encompassed grid design, docking simulations, and the precise fabrication of ligands and proteins to comprehensively analyze protein-ligand interactions inside the COX-2 binding sites.

Receptor grid generation [20]

Prior to interaction with a virtual display with waft, grid creation must be finished. The receptor's shape and properties are shown in a grid format by area, facilitating more precise scoring of ligand poses across time. Follow builds grids for each receptor conformation that experiences many states across binding to ensure that potential active compounds are not missed. Receptor grid development requires a "prepared" structure: a complete atomic structure containing suitable bond ordering and formal charges. The preparation step may often be completed automatically with the Protein Preparation Wizard [21]. RMSD values are calculated to quantify the deviation between predicted and experimental poses, with lower values indicating higher accuracy [22]. Degree RMSD For Protein Structures<1 Å: Excellent agreement (often seen in high-resolution structures). 1-2 Å: Good agreement, typically acceptable for most studies. 2-3 Å: Moderate agreement; may be acceptable depending on the context. >3 Å: Poor agreement; often indicates significant deviations.

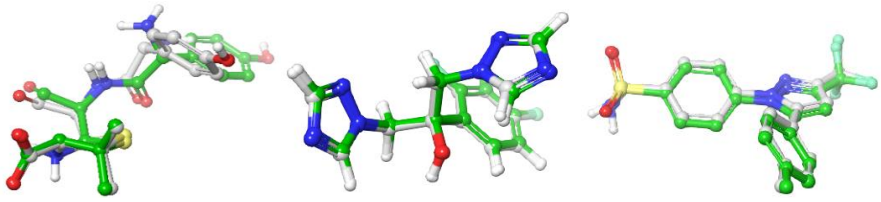

6KGV) RSMD= 2.44WMZ RSMD= 0.11176 3ln1 RSMD= 0.3385

Fig. 3: RSMD for enzymes

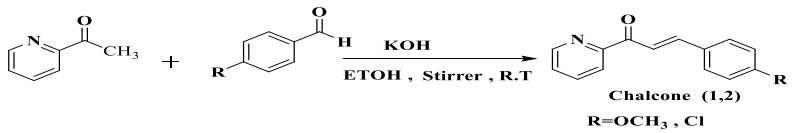

Fig. 4: Synthesis of chalcones (1-2)

Chemical synthesis

I. Step

Step one: synthesis of chalcones (1-2)

Equimolar amounts of 2-acetylpyridine (0.017 mol) and of the appropriate benzaldehydes (0.017 mol) (4-methoxybenzaldehyde, 4-chlorobenzaldehyde) were added to 100 ml of water at temperatures below 5 °C. The mixture was stirred thoroughly in order to obtain a finely dispersed emulsion for 1-2 h. (10 ml) of a 10% potassium hydroxide solution was added. The mixture was stirred for 30 min and left overnight at 4 °C. The resulting solid was filtered, washed with water, dried, and recrystallized from ethanol.

Compound (1) yellow crystals powder, yield=80%, M. P.= (90-91) °C,R_f=0.6 ATR-FTIR (υ=cm^{-1})3051, 3005(Stretchingvibrationsof CH (aromatic)), 2931(asy CH Stretchingvibrationsof CH_3), 2843(Sy CH Stretchingvibrationsof CH_3), 1662(C=O Stretchingvibrationsof*α-β* unsaturated ketone), 1593(C=N Stretching vibrations), 1566,1508(Stretchingvibrationsof aromatic and aliphatic C=C (overlapped)), 1257(C-O-C Str. Vib of C=O group aromatic C-H Bending.

Compound (2) off white powder, yield=80%, M. P.= (120-121) °C,R_f=0.5 ATR-FTIR (υ=cm^{-1})3059, 3020(Stretchingvibrationsof CH (aromatic)), 2965(Asy CH Stretchingvibrationsof CH_3), 2870(Symmetric CH Stretchingvibrationsof CH_3), 1670(C=O Stretchingvibrationsof*α-β* unsaturated ketone), 1604(C=N Stretching vibrations), 1595,1566(Stretchingvibrationsof aromatic and aliphatic C=C (overlapped)),1215 C-O-C Stretching vibrations of C=O group aromatic C-H Bending,825 N-H bending vib. Of Amine, 786(C-Cl).

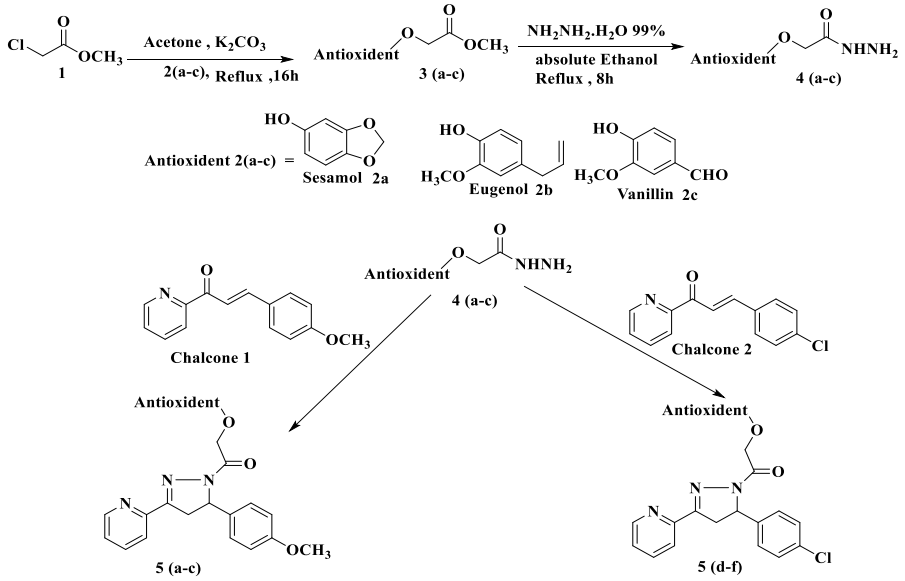

.Fig **5: Synthesize of target final compounds**

II. Step

Synthesis of antioxidant-methyl 2-chloroacetate as intermediates (included two steps)

1-Synthesize of methyl-2-phenoxyacetate

Reflux the mixture of antioxidant(sesamol, eugenol, vanillin) (0.2 mol) and methyl 2-chloropropanoate (0.2 mol) and anhydrous potassium carbonate (41.4g, 0.3 mol) in dry acetone (300 ml) on a water bath 70 °C for 16 h and hot filter the reaction mixture to remove insoluble mass. Concentrate the reaction mass under reduced pressure to obtain the product.

Compound 3a white crystalline powder Yield =75%,M. P.= (125-127) °C,R_f =0.62, ATR-FTIR) (υ =cm^{-1}): 3008 Str. VibofCH(aromatic), 2924 Asymmetric CH Stretching vibrations of CH_3, 2854 Symmetric CH Stretching vibrations of CH_3, 1743C=O Stretchingvibrationsof α-β unsaturated ketone, 1570,1508 (C=C) C=C Stretchingvibrationsof aromatic ring and 1122 C-O Stretchingthe ether (C-O) bond from the benzo[d][1,3]dioxole and the ester,752 C-OCH_3Stretching vibrations.

Compound 3b pale yellow solid, Yield=70%, M. P.= (60-62) °CR_f= 0.70 ATR-FTIR) (υ =cm^{-1}): 3183 Stretching vibrations ofCH(aromatic). 2943 Asymmetric CH Stretching vibrations of CH_3, 2835 Symmetric CH Stretching vibrations of CH_3,2727Stretching vibrations C-H aldehyde,1670 C=O Stretching vibrations of α-β unsaturated ketone, 1577and 1543 C=C Stretching vibrations of aromatic ring1226 (C-O-C) ether group,702 C-OCH_3Stretching vibrations

Compound 3c yellow crystalline solid Yield =80%, M. P.= (120-122) °C R_f =0.70, ATR-FTIR) (υ =cm^{-1}): 3050Stretching vibrations of CH(aromatic).:2960 Asymmetric CH Stretching vibrations of CH_3,2829 cm^{-1} Symmetric CH Stretching vibrations of CH_3, 2729Stretching vibrations, C-H aldehyde,1737,1674 C=O Stretching vibrations of α-β unsaturated ketone 1581.16 and 1543 C=C Stretching vibrations of aromatic ring1226 (C-O-C) C-O Str the ether (C-O) bond from the benzo[d][1,3]dioxole and the ester,702 C-OCH_3Stretching vibrations.

The synthesized compounds (5a-f) was obtained successively; the overall process for synthesizing the intermediates and targeted compounds were depicted in Scheme1. Step one Synthesis of different chalcones by classical method Claisen-Schmidt condensation reaction by two ketones with different substituted aldehyde, one ketone is 2-acetylpyridine, and different substituted aldehyde then Step Two) The reaction of the phenolic compound with methyl-2-chloroacetate to produce methyl-2-phenoxy acetate which then react with NH_2NH_2, H_2O to give methyl-2-phenoxyacetahydrazide. And Step Three Cyclization of hydrazide derivatives with methyl-2-phenoxyaceta-hydrazide hydrazide derivatives to produce pyrazoline derivatives to produce oxadiazole derivative.

2-Synthesis of 2-phenoxyacetohydrazide

Reflux the mixture of appropriate crude 2-phenoxyacetohydrazide (0.1 mol) and 5 ml of 99% hydrazine hydrate (0.1 mol) in 40 ml of ethanol in a water bath 70 °C for 8 h, then cool the reaction mixture. Collect the mixture by recrystallizing the residue from ethanol to obtain the product filtration then recrystallization of the resultant compound with petroleum ether (60-80) and ethyl acetate (25:1) (42). The R_f values were obtained from running TLC using chloroform: methanol (8.5:1.5) as the solvent system.

Compound (4a) (second step of intermediates) a yellow crystalline solid Yield =72%,M. P.= (70-72) °C R_f =0.59, ATR-FTIR) (υ =cm^{-1}): 3404 the presence of N-H bonds typical of hydrazides 3120 Stretching vibrations of CH(aromatic)and 2960 (C-H str. of CH3 and CH_2),2850 Symmetric CH Stretching vibrations of CH_3, 1651 C=O Stretching vibrationsof α-β unsaturated ketone.,. 1602and 1512 C=C Str. Stretching vibrations ring 1247 C-O Str the ether (C-O) bond from the benzo[d][1,3]dioxole and the ester, 702 C-OCH_3Stretching vibrations

Compound (4b) (second step of intermediates) light brown crystalline solid Yield =75%, M. P.= (100-102) °C R_f =0.62 ATR-FTIR) (υ =cm^{-1}): 3255 cm^{-1} (N-H stretch). 3055 C-H Stretching vibrations of CH_2,2947 Asymmetric CH Stretching vibrations of CH_3.,2920 Symmetric CH Stretching vibrations of CH_3, 2600 Stretching vibrations C-H aldehyde.1693 cm^{-1} C=O Stretching vibrations of α-β unsaturated ketone.1612,1516 C=C Stretching vibrations of aromatic ring. 1273 C-O Str the ether (C-O) bond from the benzo[d][1,3]dioxole and the ester,698 C-OCH_3Stretching vibrations

Compound (4c). ((second step of intermediates) ayellowcrystalline solid Yield =78%,M. P.= (100-102) °C R_f=0.65, ATR-FTIR) (υ =cm^{-1}):3309 the N-H Str: the primary amine (N-H) Stretching vibrations,3035. Stretching vibrations of CH(aromatic),2962 Asymmetric CH Stretching vibrations of CH_3,2916,2851 Symmetric CH Stretching vibrations of CH_3,2700 Stretching vibrations C-H aldehyde,1662 cm^{-1}C=O Stretchingvibrationsof α-β unsaturated ketone, 1616,1589,1508 C=C Stretching vibrations of aromatic ring,1238 cm^{-1}, C-O Str the ether (C-O) bond from the benzo[d][1,3]dioxole and the ester,694 C-OCH_3Stretching vibrations.

Synthesis of targeted compounds 5(a-f)

Mix one of chalcone (0.002 mol) and Synthesis of 2-phenoxyacetohydrazide (RNHNH2) (0.002 mol) in absolute ethanol (5 ml), and add potassium hydroxide (0.005 mol, 0.28 g). The mixture was heated under reflux for 8h after cooling, the separated precipitate was filtered and washed with water to obtain compounds. Recrystallization with petroleum ether (60-80) and ethyl acetate (25:1) [23]. The R_f values obtained from running TLC using (chloroform: methanol 8.5:1.5) as a solvent system

Compound (5a) 2-(benzo[d][1,3]dioxol-4-yloxy)-1-(5-(4-methoxyphenyl)-3-(pyridin-2-yl)-4,5-dihydro-1H-pyrazol-1-yl)ethan-1-one

Light yellow powder, yield=65%, M. P.= (240-245) °C, R_f=0.4 ATR-FTIR (υ =cm^{-1}3210 N-H Stretching: The primary amine (N-H) Stretching vibrations, 3050 Stretching vibrations of CH(aromatic) vibrations, 2835 Symmetric CH Stretching vibrations of CH_3.1685 C=O of α-β unsaturated ketone.1604 C=N Stretching vibrations. 1581,1508 C=C Stretching vibrations of aromatic ring. 1435 C-H Bending (Methyl) bending vibrations, 1176 C-O Str the ether (C-O) bond from the benzo[d][1,3]dioxole and the ester.

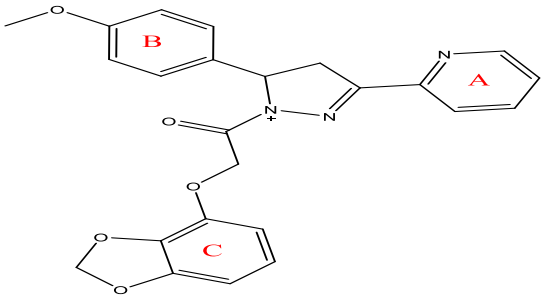

Fig. 6: Compound(5a) of final compounds

1HNMR(500 MHz, DMSOd6; δ,ppm):2.93(dd,1H, CH2-Pyrazoling ring),, 3.77 (s,3H, OCH3 group –Ring " B "), 3.82 (dd, 1H,CH2-Pyrazoling ring), 5.35 (s,2H, CH2& to O-C=O group), 5.37 (dd,1H, CH-Pyrazoling ring), 6.32 (s,2H, Methylene group of sesamol), 6.62 (d,2H, ring C), 6.92 (d,2H, ringB), 6.93 (d,1H, ring C), 7.21 (d,2H, ring B), 7.55 (complex,1H, ring A) 7.61 (complex,1H, ring A), 8.17 (d,1H, ring A), 8.50(d,1H,ring A).

13C NMR (100MHz, DMSO-d 6):(42.23)CH2 carbon of pyrazoline ring,(45.64) OCH3 group of aromatic ring " B ",(45.94) CH carbon of pyrazoline ring, (71.92)CH2& to O-C=O group, (75.80)CH of SESAMOL ring, (88.85)CH of aromatic ring (C), (101.66)CHof aromatic ring (B),(121.73)CH of aromatic ring (A),(126.28) C of aromatic ring (C), (126.51) CH of aromatic ring (A),(127.71) CH of aromatic ring (B),(134.97) C of aromatic ring (B), (136.10) CH of aromatic ring (A),(137.00) C of aromatic ring (C), (139.98) C of aromatic ring (C),(147.24) CH of aromatic ring (A), (147.98) C of aromatic ring (C), (148.26) C of aromatic ring (A),(153.08) C carbon of pyrazoline ring,(153.44) C of aromatic ring (B), (163.10 C=O group

The mass spectrum for $[M+H]^+C_{24}H_{21}N_3O_5$ m/z = 431.44 M+Fragment m/z: 58,137,252,250,264,323,

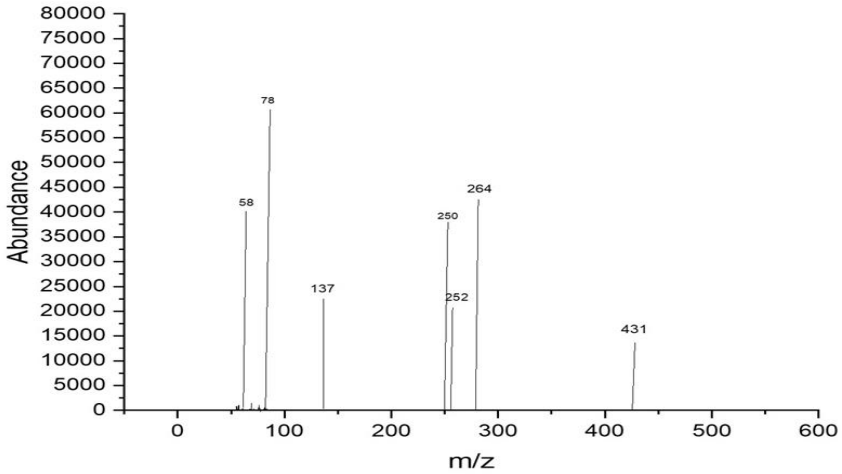

Fig. 7: The mass spectrum compound (5a)

Compound (5d) 2-(benzo[d][1,3]dioxol-4-yloxy)-1-(5-(4-chlorophenyl)-3-(pyridin-2-yl)-4,5-dihydro-1H-pyrazol-1-yl)ethan-1-one

Light white powder, yield=85%, M. P.= (230-234) °C, R_f= 0.6 ATR-FTIR (υ =cm^{-1}): 3310 N-H Stretching: The primary amine (N-H) Stretching vibrations. 3051 Stretching vibrations of CH(aromatic)vibrations,2920 Asymmetric CH Str. Vib of CH_3, 2820 Symmetric CH Stretching vibrations of CH_3.1681 C=O of α-β unsaturated ketone. 1580,1533 C=N Stretching vibrations.1580,1533 C=N Stretching vibrations. C-O-C 1191 C-O Stretching the ether (C-O-C) bond from the benzo[d][1,3]dioxole and the ester,883 C-Cl.

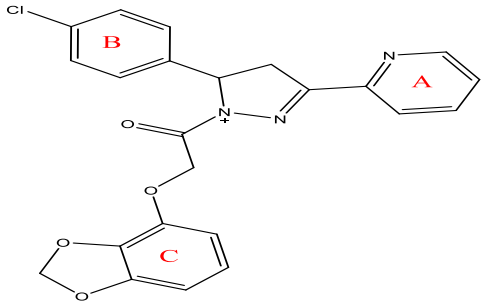

Fig. 8: Compound(5d) of final compounds

1HNMR(500 MHz, DMSOd6; δ,ppm): 3.82 (dd,1H,CH2-Pyrazoling ring), 4.09 (dd,1H, CH2-Pyrazoling ring), 5.41 (s,21H, α to C=O group), 5.44 (dd,1H, CH-Pyrazoling ring), 5.52 (s,2H, Methylene group of sesamol), 6.84 (d,2H, ring C), 6.87 (t,1H, ring C), 6.93-7.03 (m,2H, ring B), 7.12-7.19 (m,2H, ring B), 7.25 (complex,1H, ring A) 7.57 (complex,1H, ring A), 7.60(d,1H, ring A), 8.50(d,1H, ring A).

13C NMR (100MHz, DMSO-d 6):(42.71)CH2 carbon of pyrazoline ring, (54.35)CH2 carbon of pyrazoline ring, (75.81) CH2& to O-C=O group , (99.02) Methylene group of sesamol (110.89) CH of aromatic ring (C), (121.82) CH of aromatic ring (A), (126.16) CH of aromatic ring (C), (126.32) CH of aromatic ring (A), (127.08) CH of aromatic ring (B), (127.86) CH of aromatic ring (B), (128.87) C of aromatic ring (B), (136.13) CH of aromatic ring (A), (136.56) C of aromatic ring (C), (139.95) C of aromatic ring (B), (147.24) C of aromatic ring (C), (147.98) CH of aromatic ring (A), (148.26) C of aromatic ring (C), (152.98) C of aromatic ring (A), (153.41) C carbon of pyrazoline ring, (163.05) C=O group

The mass spectrum for $[M+H]^+C_{23}H_{18}ClN_3O_4$ m/z = 435.85 M^+Fragment m/z: 58,137,256,250,264,323,

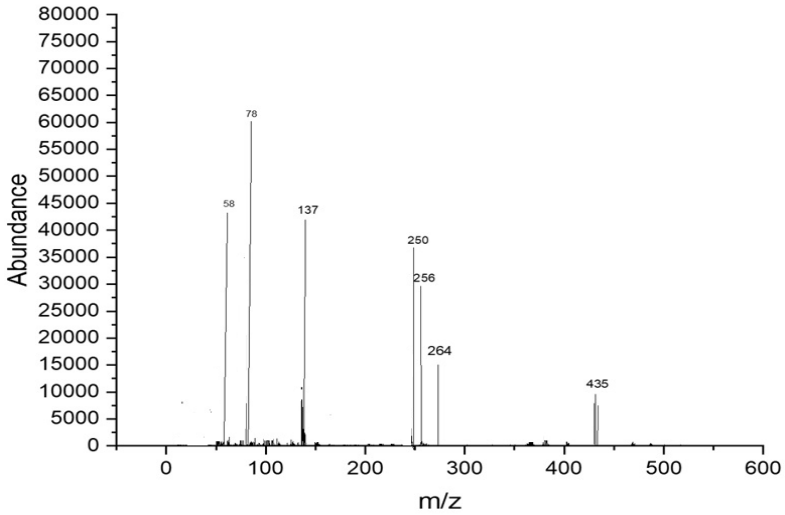

Fig. 9: The mass spectrum compound (5d)

Compound (5b) 2-(4-allyl-2-methoxyphenoxy)-1-(3-(pyridin-2-yl)-5-(p-tolyl)-4,5-dihydro-1H-pyrazol-1-yl)ethan-1-one

Light yellow powder, yield=50%, M. P.= (210-214) °C, R_f=0.45 ATR-FTIR (υ =cm^{-1}): 3320 N-H Stretching: The primary amine (N-H) O Stretching vibrations.3055 C-H Stretching vibrations of aromatic ring,2954 Asymmetric CH Stretching vibrations of CH_3, 2850 Asymmetric CH Stretching vibrations of CH_3. 1685 C=O of α-β unsaturated ketone, 1597 C=N Stretching vibrations.1581,1562 C=C Stretching vibrations of aromatic ring,1435 C-H Bending (Methyl) bending vibrations 1072 C-O-C Str the ether (C-O-C) bond from the benzo[d][1,3]dioxole and the ester.

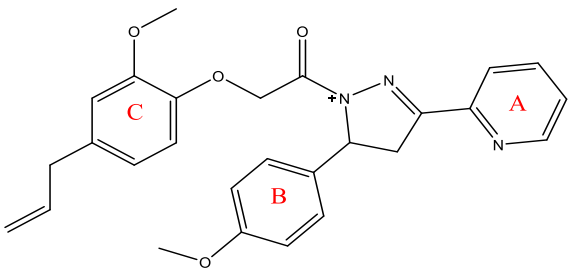

Fig. 10: Compound(5b) of final compounds

1HNMR(500 MHz, DMSOd6; δ,ppm): 2.99 (d,21H,CH2 &allylic position), 3.81(dd,1H, CH2-Pyrazoling ring), 3.90 (s,3H, OCH3 group-Ring " C "), 4.08 (s,3H,OCH3 group- Ring " B "), 4.45 (dd,1H, CH2-pyrazoline ring), 4.69 (complex,1H, Vinylic proton), 5.17(s,2H, CH2& to O-C=O group), 5.41 (ddx,1H, CH-pyrazoline ring), 5.52 (complex,1H, vinylic group), 5.75 (complex,1H, vinylic group)6.12-6.13 (m,2H, ring C), 6.41(d,1H, ring C), 6.94 (d,2H, ring B),7.21-7.29 (d,2H, ring B),7.36(complex,1H, ring A),7.56(complex,1H, ring A), 7.83(t,1H, ring A), 8.50(t,1H, ring A).

13C NMR (100MHz, DMSO-d 6):(42.16) CH2&allylic position, (45.29) CH2 carbon of pyrazoline ring, (45.45) OCH3 group of aromatic ring " B " ,(55.44) OCH3 group of aromatic ring " C " , (65.54) CH2 carbon of pyrazoline ring, (68.58) CH2& to O-C=O group , (112.42) CH of aromatic ring (C), (114.13) CH of aromatic ring (B), (120.97) CH of aromatic ring (C), (121.98) CH2 of Vinyl group , (123.78) CH of aromatic ring (A), (127.19) CH of aromatic ring (C), (129.04) CH of aromatic ring (A), (130.75) CH of aromatic ring (B) (135.60) C of aromatic ring (C), (136.24) C of aromatic ring (B), (136.70) CH of aromatic ring (A), (141.85) CH of Vinyl group , (148.06) C of aromatic ring (C), (148.51) CH of aromatic ring (A), (148.89) C of aromatic ring " C " ,(152.22) C of aromatic ring (A), (153.51) C Carbon of Pyrazoline ring ", (162.80)C of aromatic ring " B ",(168.71) C=O group

The mass spectrum for $[M+H]^+C_{27}H_{27}N_3O_4$ m/z = 457.52 M^{++}Fragment m/z: 58,147,163,252,250,264.

Compound (5e) 2-(4-allyl-2-methoxyphenoxy)-1-(5-(4-chlorophenyl)-3-(pyridin-2-yl)-4,5-dihydro-1H-pyrazol-1-yl)ethan-1-one

Pale yellow powder, yield=60%, M. P.= (220-225) °C, R_f= 0.5 ATR-FTIR (υ =cm^{-1}): 3340 N-H Stretching: The primary amine (N-H)

Stretching vibrations.3005 C-H Stretching vibrations of aromatic ring.2850 Asymmetric CH Stretching vibrations of CH_3, 1697 C=O of α-β unsaturated ketone. 1600 C=N O Stretchingvibrations.1581, 1558 C=C O Stretching vibrations of aromatic ring. 1091 C-O-C Stretching the ether. 1435 C-H Bending (Methyl) bending vibrations, 879 C-Cl.

1HNMR(500 MHz, DMSOd6; δ,ppm): 2.29 (d,2H,CH2 &allylic position), 3.63 (dd,1H, CH2-Pyrazoling ring), 3.83 (s,3H, OCH3 group- Ring " C ", 4.55(dd,1H, CH2-Pyrazoling ring), 4.68(complex,1H, Vinylic proton), 4.70 (s,2H, CH2& to O-C=O group), 5.40 (dd,1H, CH-Pyrazoling ring)), 5.41 (complex,1H, Vinylic proton),5.51(s,1H, Vinylic proton), 5.52 (complex,2H, Ring " C "), 5.53 (complex,1H, ring C), 6.99(d,2H, ring B), 7.16 (d,2H, ring B),7.34 (complex,1H, ring A),7.60(complex,1H, ring A),7.64(d,1H, ring A),8.55(d,1H, ring A).

13C NMR (100MHz, DMSO-d 6):(42.07)CH2&allylic position , (45.20) CH2 carbon of pyrazoline ring, (51.37) OCH3 group of aromatic ring " C " , (69.31)CH carbon of pyrazoline ring, (79.23)CH2& to O-C=O group , (98.76) CH of aromatic ring (C), (105.58) CH of aromatic ring (C), (120.88) CH2 of Vinyl group , (122.29) C of aromatic ring (A), (122.46 CH of aromatic ring (C), (126.82) CH of aromatic ring (A), (127.10) C of aromatic ring (B), (129.06) CH of aromatic ring (B), (130.59) C of aromatic ring (B), (136.14) C of aromatic ring (C), (136.70) CH of aromatic ring (A), (136.72) CH of Vinyl group , (139.14) C of aromatic ring (B), (141.76)C of aromatic ring (C), (148.31) CH of aromatic ring (A) (148.42) C of aromatic ring (C), (152.83) C of aromatic ring (A), (153.42) C carbon of pyrazoline ring, (162.72) C=O group

The mass spectrum for $[M+H]^+C_{26}H_{24}ClN_3O_3$ m/z = 461.93 M^{++}Fragment m/z: 58,147,163,256,250,264

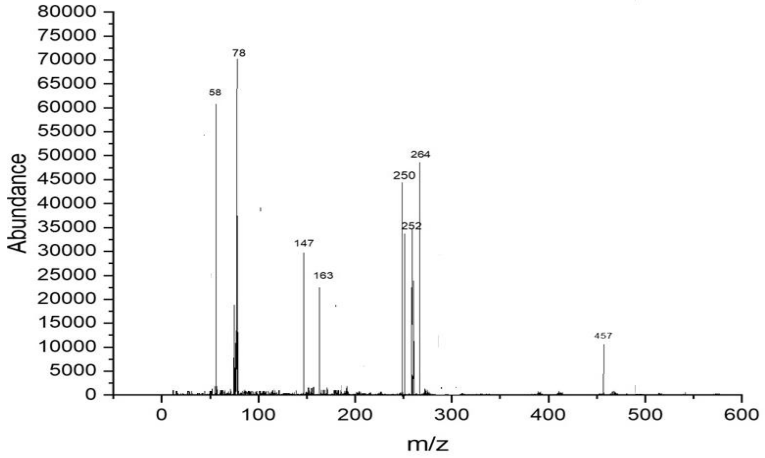

Fig. 11: The mass spectrum of compound (5b)

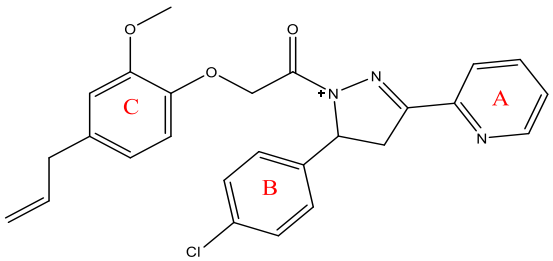

Fig. 12: Compound(5e) of final compounds

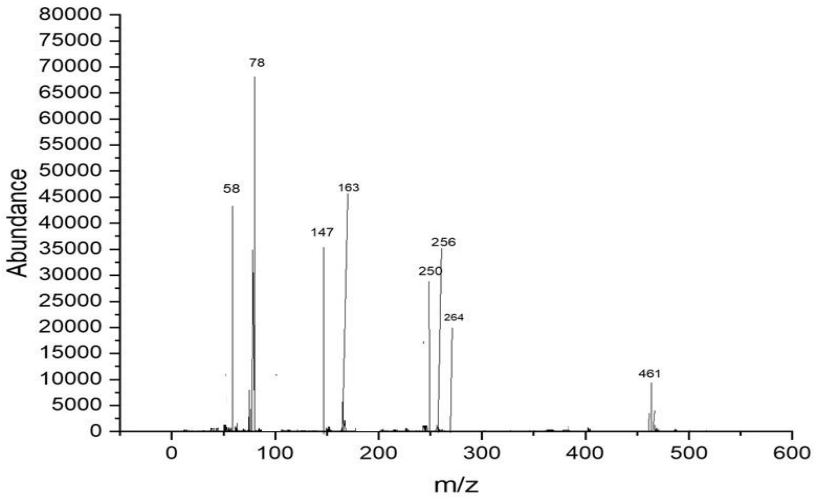

Fig. 13: The mass spectrum of compound (5e)

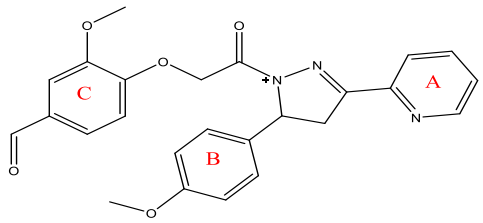

Fig. 14: Compound (5c) of final compounds

Compound (5c) 3-methoxy-4-(2-(5-(4-methoxyphenyl)-3-(pyridin-2-yl)-4,5-dihydro-1H-pyrazol-1-yl)-2-oxoethoxy)benzaldehyde

Light yellow powder, yield=60%, M. P.= (220-225) °C, R_f= 0.55 ATR-FTIR (υ =cm^{-1}): 3356 N-H Stretching: The primary amine (N-H) Stretchingvibrations.3055 C-H Stretchingvibrations of aromatic ring,2920 Asymmetric CH Stretchingvibrations of CH_3, 2850 Asymmetric CH Stretchingvibrations of CH_3. 1685 C=O of α-β unsaturated ketone1620 C=N Stretchingvibrations C-.1585,1516 C=C Stretchingvibrations of aromatic ring. 1485 C-H Bending (Methyl) bending vibrations, 1072 C-O-C Stretching the ether.

1HNMR(500 MHz, DMSOd6; δ,ppm): 3.58 (dd,1H, CH2-Pyrazoling ring), 3.69 (s,3H,OCH3 group –ring " B "), 3.72 (s,3H, OCH3 group –Ring " C "), 3.74 (dd,1H, CH2-Pyrazoling ring), 3.82 (s,2H, CH2& to O-C=O group), 4.17 (dd,1H,CH-Pyrazoling ring), 6.78(d,2H, ring B), 7.05 (d,1H, ring C), 7.25 (s,2H, ring B), 7.29(s,1H, ring C) 7.44 (d,1H, ring A), 7.79(complex,1H, ring A), 7.81 (complex,1H, ring A),7.85 (d,1H, ring A),8.57 (d,1H, ring A),8.64(s,1H, Aldehyde group).

13C NMR (100MHz, DMSO-d 6):(42.53) CH2 carbon of pyrazoline ring, (51.82) OCH3 group of aromatic ring " B " , (54.17) OCH3 group of aromatic ring " C " , (62.46) CH carbon of pyrazoline ring, (69.10) CH2& to O-C=O group , (75.63) CH of aromatic ring (C), (93.70) CH of aromatic ring (C), (119.89) CH of aromatic ring (B), (120.78) CH of aromatic ring (A), (121.62) CH of aromatic ring (C), (125.80) CH of aromatic ring (A), (126.43) CH of aromatic ring (B), (128.69) C of aromatic ring (C),(133.72) C of aromatic ring (B), (135.94) CH of aromatic ring (A), (147.73) C of aromatic ring (C), (148.06)C of aromatic ring (A), (152.81)C Carbon of Pyrazoline ring , (153.22) C of aromatic ring (B), (162.86) C=O group, (203.93) CH of C=O aldehyde

The mass spectrum for $[M+H]^+C_{25}H_{23}N_3O_5$ m/z = 445.46 M^+Fragment m/z: 58135,137,151,165,193,252.

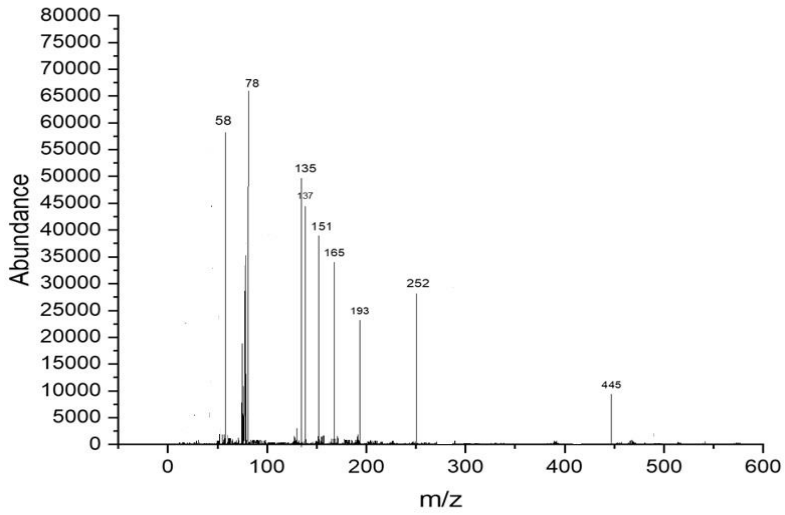

Fig. 15: The mass spectrum of compound (5c)

Compound (5f).4-(2-(5-(4 chlorophenyl)-3-(pyridin-2-yl)-4,5-dihydro-1H-pyrazol-1-yl)-2-oxoethoxy)-3 methoxybenzaldehyde

Pale yellow powder, yield=90%, M. P.= (235-238) °C,R_f= 0.8 ATR-FTIR (υ =cm^{-1}): 3348 N-H Stretching: The primary amine (N-H) Stretching vibrations. 3055 C-H Stretching vibrations of aromatic ring,2920 Asymmetric CH Stretching vibrations of CH_3,, 2850 Asymmetric CH Stretching vibrations of CH_3,1681 C=O of α-β unsaturated ketone.1620 C=N Stretching vibrations.1550,1516 C=C Stretching vibration of aromatic ring. 1415 C-H Bending (Methyl) bending vibrations,1087 C-O-C, Stretching the ether.825C-Cl.

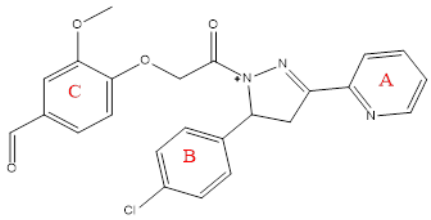

Fig. 16: Compound(5f) of final compounds

1HNMR(500 MHz, DMSOd6; δ,ppm): 3.00 (dd,1H,CH2-Pyrazoling ring), 3.82 (s,3H,OCH3 group –Ring " C "), 4.07(dd,1H, CH2-Pyrazoling ring), 5.16 (s,2H, CH2& to O-C=O group), 5. 41(dd,1H, CH-Pyrazoling ring), 6.78 (s,1H, ringC), 6.86(d,1H, ring C), 7.12 (d,2H, ring B), 7.25(s,2H, ring C), 7.29 (d,1H, ring C) 7.40 (complex,1H, ring A), 7.59(complex,1H, ring A), 7.77 (d,1H, ring A),8.51 (d,1H, ring A),8.60(s,1H,Aldehyde group).

13C NMR (100MHz, DMSO-d 6):(41.06)CH2 carbon of pyrazoline ring, (45.35)OCH3 group of aromatic ring " C " ,(55.34) CH carbon of pyrazoline ring, (68.48) CH2& to O-C=O group , (109.16) CH of aromatic ring (C), (112.32) CH of aromatic ring (C), (121.88) CH of aromatic ring (A), (123.68) CH of aromatic ring (C), (126.35) CHof aromatic ring (A), (127.09) CH of aromatic ring (B), (129.71) CH of aromatic ring (B), (130.65)C of aromatic ring (C), (135.50) C of aromatic ring (B), (136.14) CH of aromatic ring (A), (139.05) C of aromatic ring (B), (148.41) CH of aromatic ring (C), (148.71) C of aromatic ring (C), (152.12) C of aromatic ring (C), (153.41) C of aromatic ring (A), (162.02) C carbon of pyrazoline ring, (168.61) C=O group, (201.23) CH of C=O aldehyde.

The mass spectrum for $[M+H]^+C_{24}H_{20}ClN_3O_4$ m/z = 449.84 M^+Fragment m/z: 58,135,137,151,165,193,256.

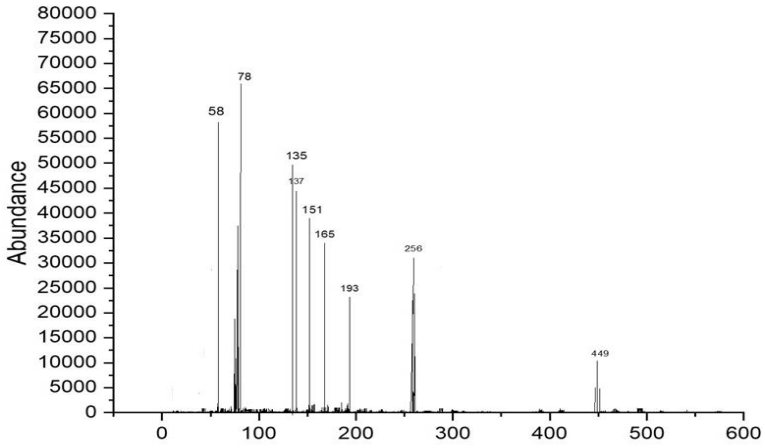

Fig. 17: The mass spectrum of compound (5f)

Pharmacological studies

Anti-inflammatory

In vivo, an albino rats were used in anti-inflammatory study, in which a reduction in paw edema thickness is the main indicator in the experimental medication for assessment activity of the synthesized compound, within the Iraqi Center for Cancer and Medical Genetics Research, sixty-six white albino rats weighing between 160 and 200g were housed. Baghdad University Animal House provided these rats. Under normal acclimation environments, the animals were fed in a commercial chaw and had free access to water. The inflammation was assessed at the beginning and during the short period of the experiment by injecting egg whites subcutaneously into the rat paw. Ten animal groups, each consisting of six rats, were present:

Group A: six rats served as control; and were treated with the vehicle (propylene glycol 50% v/v).

Group B: six rats treated with diclofenac sodium in a dose of 3 mg/kg, suspended in propylene glycol 50%

Groups (C-G): six rats per group received injections of prepared substances that were dosed and dissolved in propylene glycol as shown in table 1.

For the rats' hind paws, a 0.05 ml subcutaneous injection of an undiluted egg-white substance into the plantar side of the left hand paw may result in significant skin, discomfort because of dominating inflammation. A Vernier caliper was used to measure the paw width at intervals of 0, 30, 60, 120, 180, 240, and 300 min, respectively, following drug delivery of the desired compounds or the vehicle, thirty-minutes after the injection [23-29].

The rationale for using the egg white-induced edema model over the more standard carrageenan model lies in its specific advantages for studying inflammation. Egg white-induced edema allows for a more controlled induction of swelling, which can be crucial for certain experimental designs [30, 31]. Additionally, this model may present fewer ethical concerns, as it can potentially reduce the number of animals required for testing compared to the carrageenan model, which often necessitates multiple doses [32, 33]. In the context of animal ethics approval, it is essential to justify the choice of model based on its scientific merit and ethical implications. Researchers must demonstrate that the egg white model provides valid results while minimizing animal suffering, aligning with the principles of the animal ethics approval process [34, 35]. This careful consideration ensures compliance with ethical standards in animal research.

Calculation of the dose

The following equation [36-38] was used to calculate the recommended doses of these intended compounds:

$$\frac{\text{Dose of reference compound}}{\text{M.wt of reference compound}} = \frac{\text{Dose of tested compound}}{\text{M.wt of tested compound}}$$

Equation is used to determine the intended compounds, as indicated in table 2.

Table 1: The molecular weights and doses for Diclofenac and the intended compounds 5(a-f)

Compounds	M. wt(g/mol)	Rat dose(g/kg)
Diclofenac sodium	318.1	3
5a	431.44	4.068
5d	435.85	4.110
5b	457.52	4.314
5e	461.93	4.356
5c	445.46	4.201
5f	449.84	4.242

Antimicrobial activity

Antimicrobial activity. The minimum inhibitory concentration (MIC), alongside the agar diffusion method, was used to assess the antimicrobial activity of the final compound (5a-f) against various microorganisms, including Gram-positive bacteria (*Staphylococcus aureus* and *Streptococcus Pyogenes*) [39]. Gram-negative bacteria (*Escherichiacoli*, and *Pseudomonas. aeruginosa*), and fungi was *Candida albicans*. Standard McFarland solution (tube No. 0.5)

Standard Mcfarland solution No. 0.5 was prepared according to Baron *et al.*, 1994 as follows: Solution (A): Dissolving 1.175 g of barium chloride in 90 ml of D. W., then completed to 100 ml then Solution (B): adding 1 ml of conc. H_2SO_4 in 90 ml of D. W. and then completed to 100 ml and The two solutions were mixed by adding 0.5 ml of solution (A) to 99.5 ml of solution (B). The prepared solution was used to compare the turbidity of bacterial suspension in order to obtain an approximate cell density of 1.5×108 CFU/ml [31-34].

Minimum inhibitory concentration of reagent

The resazurin (Alamar Blue) solution was prepared by dissolving 0.015 g of resazurin in 100 ml sterile distilled water, a vortex mixer was used until well dissolved and stored at 4 °C for a maximum of one week after preparation [40]

Preparation of the culture media

All of the culture media were prepared according to the manufacturer's instructions. All these media were autoclaved at 121 °C for 15 min at 15 pounds per square inch (Psi). There were incubated for 24h at 37 °C for the sterility test and store at 4 °C until use [41]

Minimum inhibitory concentration reagent (mic)

At concentrations ranging from 10-1000 mcg/ml, several diluted solutions were created from a stock solution (10 mg/ml) of each derivative. These solutions were prepared on a microtiter plate. The use of Mueller-Hinton broth as the diluent and the inoculation with a bacterial suspension equivalent to the McFarland standard number. 0.5 (1.5×10^8 CFU/ml) is consistent with established protocols for MIC determination [24]. The addition of resazurin dye, a redox indicator that changes color in response to bacterial metabolic activity, allows for the visual determination of bacterial growth inhibition. The incubation period of 18 to 20 h at 37 °C is standard for such assays, ensuring sufficient time for bacterial growth and interaction with the antimicrobial agents. Following the incubation period, 20 µl of resazurin dye was introduced into each well. The subsequent 2-hour incubation with resazurin dye to observe color changes from blue to pink and purple provides a clear visual endpoint for determining sub-MIC concentrations, which are the lowest concentrations at which bacterial growth is inhibited but not completely eradicated [23]. Therefore, conducting an MIC test prior to the well diffusion method provides a robust foundation for understanding the effective concentration of antibiotics, facilitating more accurate and reliable antimicrobial susceptibility testing and aiding in the development of new antimicrobial agents.

Sensitivity assay

The well diffusion assay used a bacterial culture of 1.5×10^8 CFU/ml from the McFarland turbidity standard (Number 0.5). The procedure involved applying the substance to the surface of MHA plates using a swab and allowing the excess fluid to dry in a sterile hood. Four wells were created in each agar plate containing the microorganisms under examination, and 80µl of the test chemical was added to each well. The plates were then placed in an incubator at 30 °C for 72 h for fungal species and at 37 °C for 24 h for bacterial species. The zone of inhibition (ZI) width around each well was measured in millimeters to assess the antimicrobial activity [42].

Statistical analysis

All the experiments were performed and reported in triplicate. The average mean values were reported along with standard deviation values. The t-test was conducted after verifying the normality and homogeneity of the data to assess its significance and compare the means (*<0.05;**<0.01; ***<0.001). The software used for statistical analysis is R Studio 4.5, which was used for the correlations and the fig. by OriginLab2021 software.

RESULTS AND DISCUSSION

Molecular docking research provides a thorough understanding of the binding interactions of many active medicines. Tables 2,3, and 4 show the results of the molecular docking tests conducted in this study, which included nine drugs with anti-inflammatory and antibacterial prescriptions, such as diclofenac against the 3LN1 receptor, the Amoxicillin 6KGV receptor, and the antifungal 4wmz. The docking scores of the compounds were compared using *diclofenac, amoxicillin, and Fluconazole* as reference ligands, respectively. As the interaction between compounds (5a-f) for the 5KGV receptor increased, so did the ligands' affinity for 3LN1. Table 2. Anti-inflammatory Docking Scores of docked Ligands (5a-f) with (PDB Code: 3LN11), Using Diclofenac as a Reference. The interaction showed that the synthesized compound 5e and 5d produced significant results with H-bond: ARG106,TYR341, an important residue in both catalysis and binding processes. In the *in vivo* study, as illustrated in table 2 and fig. 10, all synthesized derivatives (5a-f) showed significant activity compared to the control from 2-5 h [24].

Table 2: Anti-inflammatory docking scores of docked ligands (5a-f) with (PDB Code: 3LN11), using diclofenac as a reference

ID	Docking score Kcal/mol	Types of interaction
Diclofenac	-7.367	H-Bond: HIE162,GIN108 Salt bridage: ARG83,127 Pi-Pi Stacking: TRP104,HIS119
5a	-3.694	-
5d	-7.937	H-bond: ARG106,TYR341 Pi-Pi Stacking: TYR371
5b	-7.120	H-bond: ARG106,TYR341 Pi-Pi Stacking: TRP373
5e	-8.009	H-bond: ARG106,TYR341 Halogen bond: ARG499
5c	-5.803	H-bond: ARG106,TYR341
5f	-7.156	H-bond: TYR341 Halogen bond: ARG499

Table 3: Anti-bacterial docking scores: penicillin binding protein 3 of mycobacterium tuberculosis (PDB code 6KGV), Amoxicillin as reference

ID	Docking score Kcal/mol	Types of interaction
Amoxicillin	-4.642	H-bond: GLU510,GLY505,THR433,GIN575
5a	-5.272	H-bond: THR433,GIU510 Pi-cation: ARG499 Pi-Pi Stacking TYR 574 Salt bridge: GIN 575
5d	-5.093	Pi-Pi Stacking: TYR574
5b	-5.847	2 H-bond: THR433,507 Pi-cation: ARG499,THR507 Pi-Pi Stacking TYR 574
5e	-6.111	H-bond: THR433 Pi-cation: ARG499 Pi-Pi Stacking TYR 574
5c	-5.964	Pi-cation: ARG106,499 Pi-Pi Stacking TYR 574, PHE456 Salt bridge: THR433
5f	-5.841	H-bond: THR433 Pi-cation: ARG499 Pi-Pi Stacking TYR 574, PHE456, GLY436

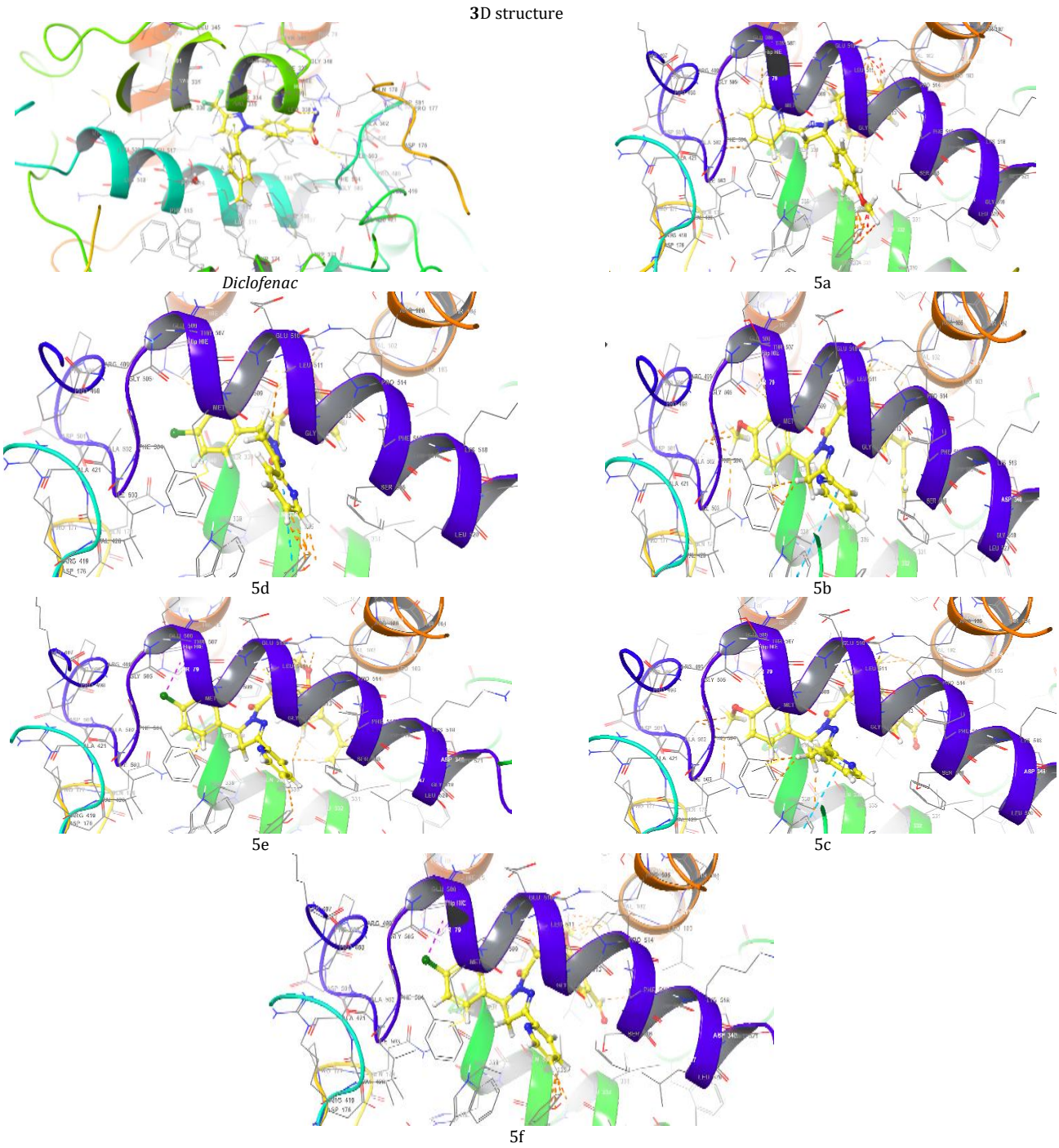

Fig. 18: Anti-inflammatory docking/3D

Table 4: Anti-fungal docking scores of docked ligands (5a-f) with (PDB code: 4WMZ), using fluconazole as a reference

ID	Docking score Kcal/mol	Types of interaction
fluconazole	-6.912	H-bond: CYS470,TYP120,H2O-OH
5a	-9.008	H-bond: CYS470 Pi-Pi Stacking: TYR126
5d	-8.279	H-bond: CYS470 Pi-Pi Stacking: TYR126
5b	-8.559	H-bond: CYS470,TYR140,H20-N
5e	-8.874	H-bond: CYS470,ILE471,TYP140
5c	-8.764	H-bond: H2O Pi-cation: LYS151
5f	-9.286	H-bond: ARG385 Pi-Pi Stacking: TYR126

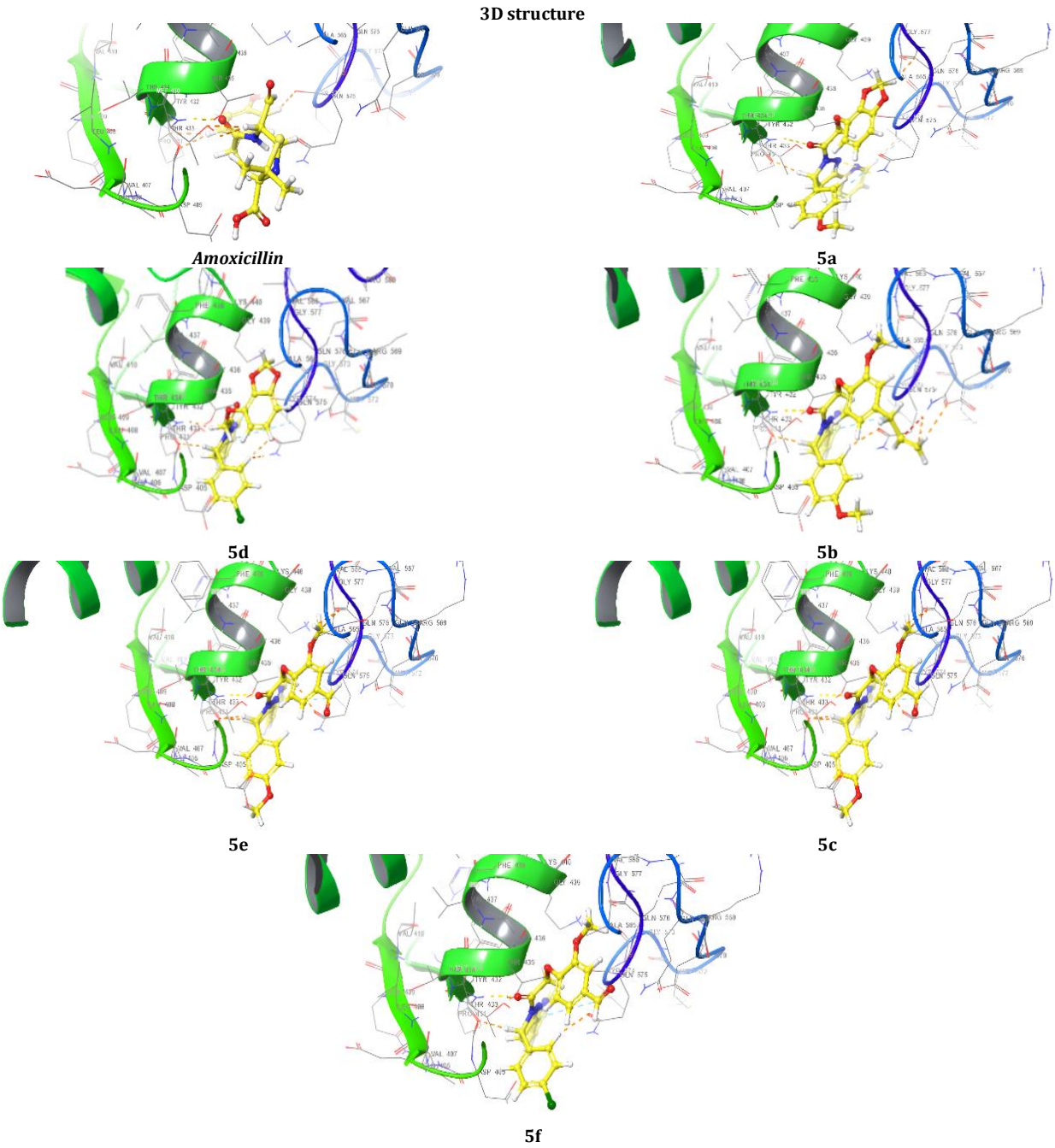

Fig. 19. Anti-bacterial docking/3D

Structure-activity relationship (SAR)

The activity of pyrazoline derivatives is highly dependent on the groups attached in various positions of the pyrazoline nuclei. For this reason, electronegative and steric factors at the N-1, C-3, and C-5 positions affect their pharmacokinetic characteristics [42].

Derivatives of the starting structure with functional groups like OCH3 and halogens like Cl increases their potential to act as inhibitors of biological targets [43].

In spite of the fact that pyrazoline derivatives possess numerous pharmacological activities, information on the therapeutic effects and toxicology are limited. Currently, the work that is being done on SARs and hybridization of their molecules recommends clearer therapeutics that are significantly safer.

Statistical test between six compounds (5a,5d,5b,5e,5c,5f and control) with times from (0 h to 5 h) (mean standard deviation)

The results presented in fig. 13 and table 5, paw thickness was measured at different time intervals from zero to five hours for the six compounds (5a,5d,5b,5e,5c and 5f). The highest paw thickness was observed at 6.6 mm after half an hour, followed by a similarly high value of 6.5 mm after two hours, indicating a strong inflammatory response during this period. Statistical analysis using One-Way ANOVA (table 5) revealed very highly significant differences ($p<0.0002$) in paw thickness from zero to two hours, while the significance remained high but slightly reduced from three to five hours, with p-values ranging from 0.001 to 0.003. These findings suggest that the compounds induce a pronounced inflammatory response within the first two hours, which gradually diminishes over time. The highly significant p-values highlight the robustness of the observed differences and underscore the temporal dynamics of the inflammatory response induced by these compounds. n= 6 animals no. NS: No Significant Value (*<0.05;**<0.01; ***<0.001).

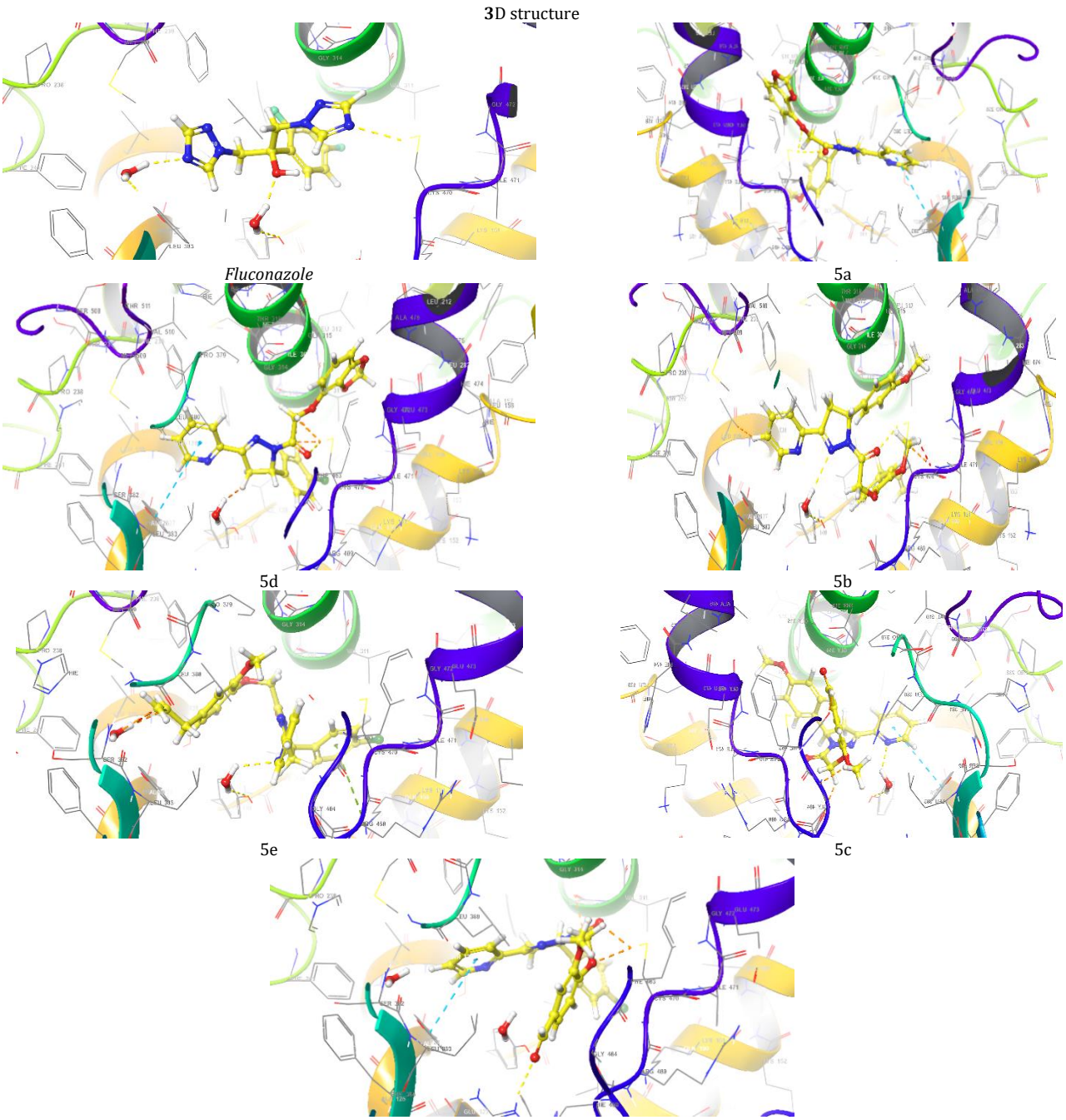

Fig. 20: Anti-FUNGICAL docking/3D

Table 5: Statistical test between six compounds (5a,5d,5b,5e,5c,5f and control) with times from (Zero hour to 5 h) (mean standard deviation)

Time							
Compounds	**0 h**	**0.5 h**	**1 h**	**2 h**	**3h**	**4h**	**5h**
Control	4.44±0.03	4.63±0.02	5.97±0.03	7.58±0.5	7.67±0.03	6.89±0.02	6.48±0.11
Standard	4.35±0.02	4.49±0.02	5.91±0.04	6.26±0.02	6.02±0.01	5.74±0.01	5.16±0.02
5a	4.41±0.01	4.56±0.02	5.88±0.04	6.07±0.01	5.86±0.03	5.67±0.02	5.06±0.01
5d	4.42±0.01	4.65±0.02	5.01±0.03	6.2±0. 02	5.98±0.04	5.73±0.01	5.13±0. 02
5b	4.43±0.02	4.56±0.02	5.86±0.03	6.52±0.01	6.37±0.01	6.17±0.03	5.67±0.01
5e	4.48±0.02	4.62±0.02	5.91±0.03	6.28±0.01	6.02±0.01	5.77±0.02	5.19±0. 01
5c	4.39±0.01	4.58±0.01	5.9 ±0.03	6.9±0.04	6.82±0.01	6.64±0.02	6.11±0.02
5f	4.43±0.02	4.57±0.02	5.86±0.03	6.23±0.01	5.97±0.01	5.72±0.02	5.14±0.01
Mean±SD	4.42±0.04	6.6±0.05	5.8±0.3	6.5±0.5	6.34±0.6	6.04±0.6	5.5±0.6
SEM	0.013	0.02	0.1	0.2	0.22	0.3	0.2
P-value	0.0006***	0.0003***	0.0002***	0.003**	0.001**	0.003**	0.001**

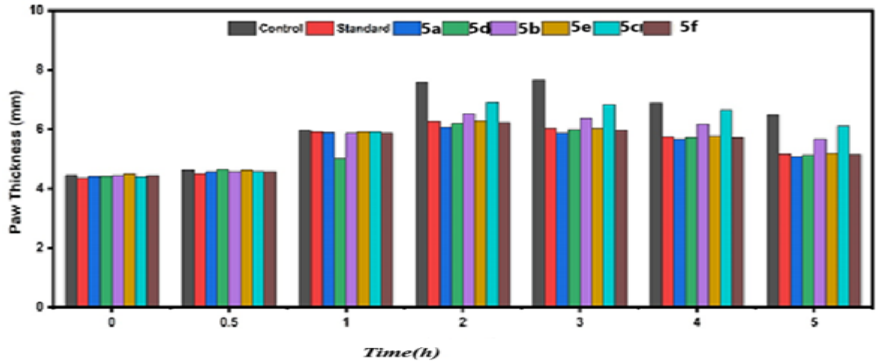

Fig. 21: The histogram of six compounds (5a,5d,5b,5e,5c,5f and control) with times from (Zero hour to 5 h)and mean paw thickness(mm). (mean standard deviation)

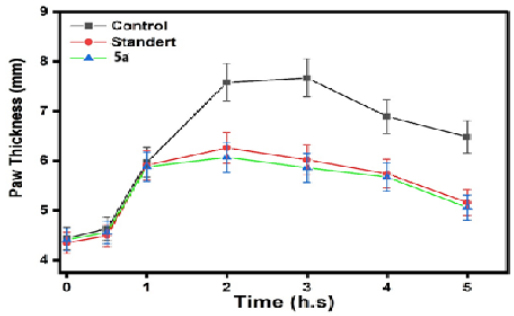

Fig. 22: Anti-inflammatory of control and standard with the compounds (5a)

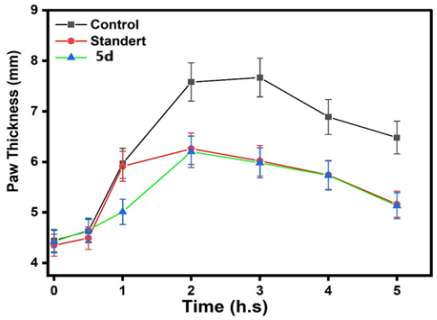

Fig. 23: Anti-inflammatory of control and standard with the compounds (5d)

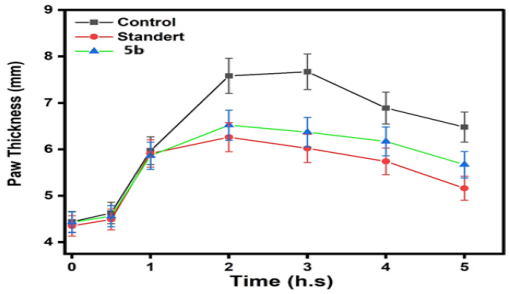

Fig. 24: Anti-inflammatory of control and standard with the compounds (IIId)

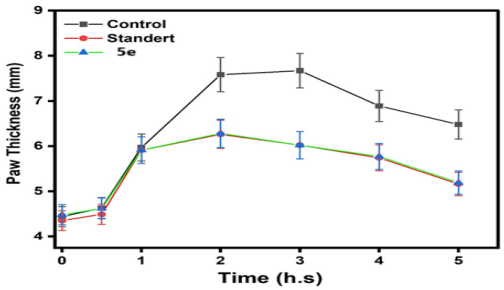

Fig. 25: Anti-inflammatory of control and standard with the compounds (5e)

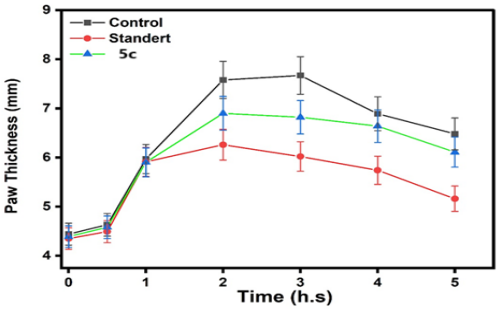

Fig. 26: Anti-inflammatory of control and standard with the compounds (5c)

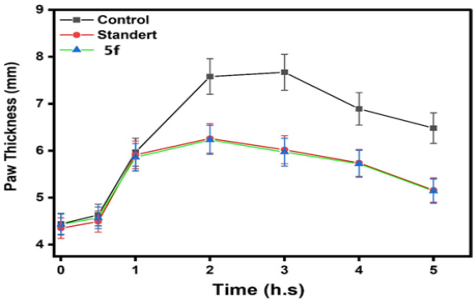

Fig. 27: Anti-inflammatory of control and standard with the Compounds (5f)

This fig. 22 compares the anti-inflammatory effects of the control, standard, and Compound (5a). The activity of Compound 5a was lower than that of both the control and the standard. This fig. 23 compares the anti-inflammatory effects of the control, standard, and Compound (5d). The activity of Compound 5d was lower than that of both the control and the standard. This fig. 24 illustrates the anti-inflammatory effects of the control, standard, and Compound (5b). The activity of Compound 5d falls within the range observed for both the control and the standard. This fig. 25 illustrates the anti-inflammatory effects of the control, standard, and Compound (5e). The activity of Compound 5e falls within the range observed for both the control and the standard. This fig. 26 illustrates the anti-inflammatory effects of the control, standard, and Compound (5c). The activity of Compound 5c falls within the range observed for both the control and the standard. This fig. 27 compares the anti-inflammatory effects of the control, standard, and Compound (5f). The activity of Compound 5f was lower than that of both the control and the standard.

Table 6: Pairwise comparisons of antimicrobial activity across compounds and microbial strains

Microbial strain	Comparison	Z-value	P-Value	Significant
Staphylococcus aureus	Amoxicillin vs DMSO	4.521	<0.001	***
	Ciprofloxacin vs DMSO	4.312	<0.001	***
	Amoxicillin vs 5a	3.871	0.001	**
Streptococcus pyogenes	Ciprofloxacin vs DMSO	4.210	<0.001	***
	5d vs DMSO	3.781	0.002	**
Escherichia coli	Ciprofloxacin vs DMSO	4.052	<0.001	***
	5b vs DMSO	3.765	0.002	**
Pseudomonas aeruginosa	Ciprofloxacin vs DMSO	3.892	<0.001	***
	5d vs DMSO	3.451	0.002	**
Candida albicans	Fluconazole vs DMSO	4.672	<0.001	***
	Fluconazole vs Amoxicillin	4.521	<0.001	***

The analysis reveals distinct antimicrobial profiles: amoxicillin and ciprofloxacin show broad-spectrum antibacterial activity (p<0.001 vs DMSO), while fluconazole exhibits exclusive antifungal action against C. albicans (p<0.001). Novel compounds 5d and 5b demonstrate selective efficacy against Gram-positive pathogens (p<0.01), with 5f showing specific activity against *S. aureus. P. aeruginosa* displays characteristic resistance to *non-fluoroquinolones*, while all compounds remain ineffective against non-target pathogens (p>0.05). These results validate known mechanisms of established drugs and highlight promising narrow-spectrum candidates for further development, while confirming appropriate negative controls (DMSO, p<0.05 in all valid comparisons). Only significant comparisons (p<0.05) are shown.***p<0.001, **p<0.01

Table 7: *In silico* ADME prediction results of the final compounds 5(a-f)

Com	Mol. wt	Donor HB	Accept HB	QPlogP o/w	CNS	Rule of three	Rule of five	% Human oral absorption
5a	431.447	0.000	7.500	4.141	0	0	0	100.000
5d	435.866	0.000	6.750	4.365	1	0	0	100.000
5b	457.528	0.000	6.750	5.858	0	1	2	100.000
5e	461.947	0.000	6.000	6.290	0	1	2	100.000
5c	445.474	0.000	8.750	3.841	-2	0	1	100.000
5f	449.893	0.000	8.000	4.026	-1	0	0	100.000
Recommended values	130-725	0-6	2-20	-2-6.5	–2 (inactive) to+2 (active) scales	QPlogS>-5.7(Solubility)	Max4	>80% is high <25% is poor

PSA:-5c (101.420), and 5f (101.3332) give high results. Hydrogen bond acceptor 5c (8.750), 5f (8.000) and 5a (7.500) give the highest results. QPlogP o/w:-5e (6.290), 5b (5.858), and 5d (4.365) give the highest results. Rule of Five:-All the compounds within the acceptable value with Lipinski's rule of five. %Human oral absorption:-all the synthesized compounds give good results

Antibacterial activity

Using a well penetrated diffusion type approach, the anti-microbial activity of the synthesized final compounds (5a-f) against g-negative and g-positive bacteria as well as anti-fungi (*fluconazole* is a reference product) was evaluated. The antibacterial solubilizer was a combination of *ciprofloxacin and amoxicillin*. The solvent and control were DMSO.

Minimum inhibitory concentration (MIC)

Bacterial susceptibility to antibiotics was assessed using a rapid resazurin microtiter test method. Compounds 5(a-f), *amoxicillin,* and *Ciprofloxacin* were produced in a microtiter plate using Mueller-Hinton broth in double serial dilutions. A total of 1000, 500, 250, 125, and 64.5 µg/ml were examined. Twenty microliters of bacterial suspension (1.5×10^8 CFU/ml) were added to each well, with the exception of the negative control. For 18 to 20 h, plates were incubated at 37 °C. To see color changes, 20 µl of resazurin dye was applied to each well and incubated for two hours. The lowest concentrations at which the color changed from blue to pink and purple, signifying suppression of bacterial growth, were determined to be the sub-MIC values (table 8) [44].

Table 8: MIC values for pyrazolin derivatives (5a-f); *ciprofloxacin, amoxicillin,* and *fluconazole as* standard

Compounds	MIC (mm)				
	Gram-positive bacteria		Gram-negative bacteria		Fungi
	Staphylococcus. aureus	*Streptococcus. Pyogenes*	*Escherichia. coli*	*Pseudomonas. aeruginosa*	*Candida albicans*
	Conc.(µcg/ml)				
Amoxicillin	125	250	125	250	
Ciprofloxacin	125	125	125	125	
Fluconazole	-	-	-	-	125
		-	-		
DMSO	*as a solvent and controlas a solvent and controlas a solvent and control*				
5a	64.5	-	64.5	64.5	64.5
5d	-	-	64.5	64.5	-
5b	64.5	64.5	64.5	64.5	64.5
5e	64.5	64.5	64.5	-	-
5c	64.5	64.5	64.5	64.5	64.5
5f	64.5	64.5	64.5	64.5	64.5

Inhibition zone determination

The agar well diffusion method was employed to assess the antibacterial activity of the compounds 5(a-f) against *Staphylococcus. Aureus (S. aureus), Streptococcus. Pyogenes (S. pyogenes), Escherichia. Coli (E. coli), Pseudomonas aeruginosa (P. aeruginosa)* isolates were grown in nutrient broth and incubated at 37 °C for 18–24 h. A bacterial suspension with moderate turbidity (1.5×10^8 CFU/ml) was prepared, and 0.1 ml was spread on nutrient agar plates. After drying for 10 min, 5 mm diameter wells were created in the agar. Each well was filled with 50 µl of the test materials at concentrations equal to the MIC values obtained from the Minimum Inhibitory Concentration (MIC) (table 9).

Table 9: Statistical test between six compounds (5a, 5d, 5b, 5e, 5c, 5f) and zone of inhibition (mean standard deviation)

Compounds	*Staphylococcus. aureus*	*Streptococcus. Pyogenes*	*Escherichia. coli*	*Pseudomonas. aeruginosa*	*Candida albicans*
Amoxicillin	40	38	39	37	-
Ciprofloxacin	39	35	33	32	-
Fluconazole	-	-	-	-	36
DMSO	-	-	-	-	-
5a	15	23	29	24	25
5d	22	32	23	28	32
5b	31	25	33	25	31
5e	23	25	24	20	26
5c	25	20	18	20	13
5f	30	28	29	19	28
Mean±SD	28.1±8.59	28.3±6.23	28.5±6.7	25.63±6.4	27.3±7.3
SEM	3.04	2.2	2.4	2.3	2.3
P-value	0.0003***	0.00004***	0.00006***	0.00009***	0.0006***

Based on the results presented in fig. 14, the zone of inhibition for the six compounds (**5**a, 5d, 5b, 5e, 5c and 5f) ranged from 25 to 28 µcg/ml, indicating moderate antimicrobial activity against the tested microorganisms. Statistical analysis using One-Way ANOVA (table 9) revealed very highly significant differences ($p<0.0003$) in the antimicrobial efficacy of the compounds (Amoxicillin, Ciprofloxacin, Fluconazole, DMSO, (5a,5d,5b,5e,5c and 5f) across the tested pathogens, including *Staphylococcus aureus, Streptococcus pyogenes, Escherichia coli, Pseudomonas aeruginosa,* and *Candidaalbicans*. These findings suggest that the compounds exhibit varying degrees of antimicrobial activity, with some demonstrating broad-spectrum efficacy. The high statistical significance ($p<0.0003$) underscores the robustness of the observed differences and highlights the potential of these compounds as candidates for further antimicrobial development. The results align with established methodologies for evaluating antimicrobial activity, as described by Bauer *et al.* (1966), and emphasize the need for further investigation into the mechanisms of action and clinical potential of these compounds. NS: No Significant Value (*<0.05;**<0.01; ***<0.001)n= 8.

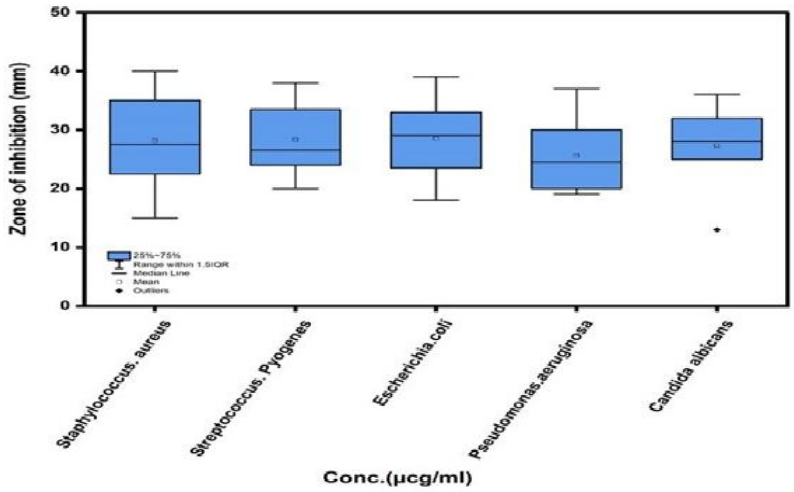

Fig. 28: The boxplot of zone of inhibition (5a,5d,5b,5e,5c, 5f) and the isolations

The Tukey HSD analysis revealed that 5c exhibited significantly stronger and more sustained effects than Standard at critical 2-3 h timepoints ($p<0.01$), while Control showed expected peak responses at 2h ($p<0.001$). Notably, 5c maintained superior activity over both Standard and 5b during the key 2-3h treatment window (mean differences+0.45 to+0.64), with all compounds displaying characteristic time-dependent response patterns that diminished by 5h. These results identify 5c as the most promising candidate, demonstrating both rapid onset (significant by 2h) and prolonged duration of action compared to reference compounds

The synthesis and evaluation of new pyrazoline derivatives bearing pyridine ring scaffolds have shown promising results in various pharmacological applications, particularly in anti-inflammatory activities and antimicrobial, Molecular docking studies have been pivotal in predicting the binding affinities and interactions of these compounds with target proteins. The paper focuses on synthesizing pyrazoline-thiazole hybrids and their bio-evaluation against α-glucosidase and urease, revealing potent inhibitory activities. However, it does not provide a discussion or comparison with other studies on in silico molecular docking of pyridine derivatives [45]. The paper discusses the synthesis and pharmacological evaluation of 1,3,5-Pyrazoline derivatives, highlighting compound IVh's significant antidepressant and antioxidant activities. However, it does not provide a comparison with other studies or specific references regarding in silico molecular docking [46]. The paper focuses on the design,

synthesis, and pharmacological evaluation of new pyrazoline derivatives targeting cyclooxygenase enzymes, but does not provide a discussion comparing results with other studies or specific references related to *in silico* molecular docking of pyridine ring scaffolds [47].

Table 10: Significant pairwise comparisons from Tukey HSD post-hoc analysis of compound effects over time

Comparison	Time (h)	Mean difference	p-value	Effect size (η^2)
Between compounds				
Control vs. Standard	2	+1.32	<0.001	0.42
Control vs. 5c	2	+0.68	0.003	0.18
5c vs. Standard	2	+0.64	0.007	0.15
Control vs. Standard	3	+1.65	<0.001	0.51
5c vs. 5b	3	+0.45	0.028	0.09
Within compounds				
Control: 2h vs. 0h	-	+3.14	<0.001	0.72
Control: 2h vs. 1h	-	+1.61	<0.001	0.38
5c: 2h vs. 0h	-	+2.51	<0.001	0.64
5c: 2h vs. 5h	-	+0.79	0.012	0.22

-Only significant comparisons ($p<0.05$) shown.
-Effect sizes calculated as partial eta-squared (η^2), with thresholds: 0.01 (small), 0.06 (medium), 0.14 (large).
-Directionality: "+" indicates first group>second group in comparison.
-Time points reflect hours post-treatment.

ACKNOWLEDGMENT

The authors are grateful to the College of Pharmacy/University of Baghdad; the authors declare that they have no received financial support from an Institution.

CONCLUSION

the synthesis of new pyrazoline derivatives 5(a-f) through derivatives bearing heterocyclic scaffolds (a-i) were successfully synthesized and their physical properties (melting point, description and R_f) have been checked, also they were characterized by spectral data (FTIR, 1HNMR, 13 C NMR and Mass spectrometry) and the docking investigation showed that more of the newly synthesized derivatives had better active site alignment. The virtual ADME tests also show acceptable pharmacokinetic features, and *in vivo* anti-inflammatory evaluation of the synthesized compounds produced a reduction in the paw edema thickness; the effect was comparable to that of the reference drug (diclofenac sodium). All the prepared compounds showed different results, ranging from high activity, moderate activity, hardly activity to inactive sructures were consistent with the data The evaluation of the final compounds, the final synthesized derivatives 5(a-f) demonstrated superior antibacterial activity, exhibiting significant antibacterial activity give all low dose against g-negative bacteria *Escherichia. coli(Escherichia coli)* compared to the reference drug (Amoxicillin and ciprofloxacin) Comparing chemical compound(5a,5d,5b,5e,5c and 5f) to MIC more compound give activity low dose, the MIC findings demonstrate that it can inhibit several bacterial strains at low doses.

FUNDING

The writers herein affirm that they have not been compensated in any way by any institution.

ETHICS STATEMENTS

The authors declare that their study does not need ethical approval from an ethics committee.

AUTHORS CONTRIBUTIONS

The research project was designed by both authors, and their contributions extended to the research approach, which they put into practice by preparing target compounds for FTIR and 1HNMR testing and interpreting the results. Both writers not only conducted and discussed antibacterial and anti-inflammatory tests, but they also assessed the whole study paper for scientific rigor and language use.

CONFLICTS OF INTERESTS

The writers of this paper affirm that they are free from any ties or financial conflicts of interest that may have seemed to impact their work.

REFERANCES

1. Salum KA, Alidmat MM, Khairulddean M, Kamal NN, Muhammad M. Design synthesis characterization and cytotoxicity activity evaluation of mono-chalcones and new pyrazolines derivatives. J Appl Pharm Sci. 2020;10(8):20-36. doi: 10.7324/JAPS.2020.10803.
2. Younus ZG, Omar T. Synthesis, characterization and evaluation of antioxidant activity of new pyrazolines derivatives. J Res Med Dent Sci. 2023;11(1):82-9.
3. Kumari S, Paliwal SK, Chauhan R. An improved protocol for the synthesis of chalcones containing pyrazole with potential antimicrobial and antioxidant activity. Curr Bioact Compd. 2018;14(1):39-47. doi: 10.2174/1573407212666161101152735.
4. Vasquez Martinez YA, Osorio M, San Martin D, Carvajal M, Vergara A, Sanchez E. Antimicrobial anti-inflammatory and antioxidant activities of polyoxygenated chalcones. J Braz Chem Soc. 2018;30(2):286-304. doi: 10.21577/0103-5053.20180177.
5. Jain SK, Singhal R, Jain NK. Synthesis, characterization and biological activity of pyrazoline derivatives. Res J Pharm Technol. 2021;14(12):6223-7. doi: 10.52711/0974-360X.2021.01077.
6. Najmuldeen ZD, Omar TN. Synthesis characterization and evaluation of new pyrazoline derivatives containing sulfonamide moiety as antimicrobial and anti-inflammatory agents. J Res Med Dent Sci. 2023;11(1):73-81.
7. Mantzanidou M, Pontiki E, Hadjipavlou Litina D. Pyrazoles and pyrazolines as anti-inflammatory agents. Molecules. 2021;26(11):3439. doi: 10.3390/molecules26113439, PMID 34198914.
8. Parajuli RR, Pokhrel P, Tiwari AK, Banerjee J. Pharmacological activities of pyrazolone derivatives. J Appl Pharm Res. 2013;1(1):5-13.
9. Sabah RS, Al Garawi ZS, Al Jibouri MN. The utilities of pyrazolines encouraged synthesis of a new pyrazoline derivative via ring closure of chalcone for optimistic neurodegenerative applications. MJS. 2022;33(1):21-31. doi: 10.23851/mjs.v33i1.1067.
10. Vasudha D, Jagadeesh A, Mali SN, Bhandare RR, Shaik AB. Synthesis, molecular docking and pharmacological evaluations of novel naphthalene pyrazoline hybrids as new orally active anti-inflammatory agents. Chem Phys Impact. 2024 Jun;8:100500. doi: 10.1016/j.chphi.2024.100500.
11. Bendi A, Devi P, Sharma H, Yadav G, Raghav N, Pundeer R. Innovative pyrazole hybrids: a new era in drug discovery and synthesis. Chem Biodivers. 2025;22(4):e202402370. doi: 10.1002/cbdv.202402370, PMID 39613478.
12. Nair AB, Dalal P, Kadian V, Kumar S, Garg M, Rao R. Formulation strategies for enhancing pharmaceutical and nutraceutical potential of sesamol: a natural phenolic bioactive. Plants (Basel). 2023;12(5):1168. doi: 10.3390/plants12051168, PMID 36904028.

13. Kaufman TS. The multiple faces of eugenol a versatile starting material and building block for organic and bio-organic synthesis and a convenient precursor toward bio-based fine chemicals. J Braz Chem Soc. 2015 Jun;26(6):1055-85. doi: 10.5935/0103-5053.20150086.
14. Kafali M, Finos MA, Tsoupras A. Vanillin and its derivatives: a critical review of their anti-inflammatory anti-infective wound healing neuroprotective and anti-cancer health promoting benefits. Nutraceuticals. 2024;4(4):522-61. doi: 10.3390/nutraceuticals4040030.
15. Stanzione F, Giangreco I, Cole J. Chapter four use of molecular docking computational tools in drug discovery. Prog Med Chem. 2021 Jan;60:273-343. doi: 10.1016/bs.pmch.2021.01.004.
16. Biondo C. Bacterial antibiotic resistance: the most critical pathogens. Pathogens. 2023;12(1):116. doi: 10.3390/pathogens12010116, PMID 36678464.
17. Larsson DG, Flach CF. Antibiotic resistance in the environment. Nat Rev Microbiol. 2022;20(5):257-69. doi: 10.1038/s41579-021-00649-x, PMID 34737424.
18. Yang Y, Yao K, Repasky MP, Leswing K, Abel R, Shoichet BK. Efficient exploration of chemical space with docking and deep learning. J Chem Theor Comput. 2021;17(11):7106-19. doi: 10.1021/acs.jctc.1c00810, PMID 34592101.
19. Lu C, Wu C, Ghoreishi D, Chen W, Wang L, Damm W. OPLS4: improving force field accuracy on challenging regimes of chemical space. J Chem Theory Comput. 2021;17(7):4291-300. doi: 10.1021/acs.jctc.1c00302, PMID 34096718.
20. Zhong HA, Almahmoud S. Docking and selectivity studies of covalently bound janus kinase 3 inhibitors. Int J Mol Sci. 2023;24(7):6023. doi: 10.3390/ijms24076023, PMID 37047004.
21. Qin HL, Zhang ZW, Ravindar L, Rakesh KP. Antibacterial activities with the structure activity relationship of coumarin derivatives. Eur J Med Chem. 2020 Dec 1;207:112832. doi: 10.1016/j.ejmech.2020.112832, PMID 32971428.
22. Ballante F, Marshall GR. An automated strategy for binding pose selection and docking assessment in structure based drug design. J Chem Inf Model. 2016;56(1):54-72. doi: 10.1021/acs.jcim.5b00603, PMID 26682916.
23. Redasani VK, Bari SB. Synthesis and evaluation of mutual prodrugs of ibuprofen with menthol thymol and eugenol. Eur J Med Chem. 2012 Oct;56:134-8. doi: 10.1016/j.ejmech.2012.08.030, PMID 22982120.
24. Fayez N, Khalil W, Abdel Sattar E, Abdel Fattah AM. *In vitro* and *in vivo* assessment of the anti-inflammatory activity of olive leaf extract in rats. Inflammopharmacology. 2023;31(3):1529-38. doi: 10.1007/s10787-023-01208-x, PMID 37029328.
25. Zhuang C, Zhang W, Sheng C, Zhang W, Xing C, Miao Z. Chalcone: a privileged structure in medicinal chemistry. Chem Rev. 2017;117(12):7762-810. doi: 10.1021/acs.chemrev.7b00020, PMID 28488435.
26. Edwards RA, Easteal AJ, Gladkikh OP, Robinson WT, Turnbull MM, Wilkins CJ. A reversible non-disruptive phase transition shown by the zinc iodide dimethylformamide complex ZnI_2 (dmf)2. Acta Crystallogr B Struct Sci. 1998;54(5):663-70. doi: 10.1107/S0108768198000536.
27. Raauf AM, Omar TN, Mahdi MF, Fadhil HR. Synthesis molecular docking and anti-inflammatory evaluation of new trisubstituted pyrazoline derivatives bearing benzenesulfonamide moiety. Nat Prod Res. 2024;38(2):253-60. doi: 10.1080/14786419.2022.2117174, PMID 36047992.
28. Omar TN. Synthesis of schiff bases of benzaldehyde and salicylaldehyde as anti-inflammatory agents. Iraqi J Pharm Sci. 2007;16(2):17-1. doi: 10.31351/vol16iss2pp5-11.
29. Kanaan S, Omar TN. Synthesis and preliminary anti-inflammatory and anti-microbial evaluation of new 4, 5-dihydro-1H-pyrazole derivatives. Iraqi J Pharm Sci. 2023;32(Suppl):262-70. doi: 10.31351/vol32issSuppl.pp262-270.
30. Barung EN, Dumanauw JM, Duri MF, Kalonio DE. Egg white induced inflammation models: a study of edema profile and histological change of rats paw. J Adv Pharm Technol Res. 2021;12(2):109-12. doi: 10.4103/japtr.JAPTR_262_20, PMID 34159139.
31. Webb DR. Animal models of human disease: inflammation. Biochem Pharmacol. 2014;87(1):121-30. doi: 10.1016/j.bcp.2013.06.014, PMID 23811309.
32. Morris CJ. Carrageenan induced paw edema in the rat and mouse. Methods Mol Biol. 2003;225:115-21. doi: 10.1385/1-59259-374-7:115, PMID 12769480.
33. Olsson IA, Nielsen BL, Camerlink I, Pongracz P, Golledge HD, Chou JY. An international perspective on ethics approval in animal behaviour and welfare research. Appl Anim Behav Sci. 2022 Aug;253:105658. doi: 10.1016/j.applanim.2022.105658.
34. Suh HR, Cho HY. Reduction of edema and pain in transcutaneous electrical nerve stimulation treated arthritic rat. Tohoku J Exp Med. 2024;262(4):245-52. doi: 10.1620/tjem.2024.J006, PMID 38267059.
35. Azilagbetor DM, Shaw D, Elger BS. Animal research regulation: improving decision making and adopting a transparent system to address concerns around approval rate of experiments. Animals (Basel). 2024;14(6):846. doi: 10.3390/ani14060846, PMID 38539944.
36. Tagreed NA, Omar A. Synthesis and preliminary pharmacological evaluation of esters and amides derivatives of naproxen as potential anti-inflammatory agents. Iraqi J Pharm Sci. 2013;22(1):120-7.
37. K MM, T Omar. Synthesis characterization and preliminary pharmacological eva-luation of new 2-pyrazoline derivatives derived from resorcinol. J Popul Ther Clin Pharm Macol. 2023;30(14):319-26. doi: 10.47750/jptcp.2023.30.14.042.
38. Al Nakeeb MR, Omar TN. Synthesis characterization and preliminary study of the anti-inflammatory activity of new pyrazoline containing ibuprofen derivatives. Iraqi J Pharm Sci. 2019;28(1):131-7. doi: 10.31351/vol28iss1pp131-137.
39. Abdul A. Synthesis of some prodrug compounds depending on maleimide derivatives method. J Chem Soc Pak. 2023;45(5)460-73. doi: 10.52568/001335/JCSP/45.05.2023.
40. Elshikh M, Ahmed S, Funston S, Dunlop P, McGaw M, Marchant R. Resazurin based 96-well plate microdilution method for the determination of minimum inhibitory concentration of biosurfactants. Biotechnol Lett. 2016;38(6):1015-9. doi: 10.1007/s10529-016-2079-2, PMID 26969604.
41. Henshaw P. Use of alamarBlue as an indicator of microbial growth in turbid solutions for antimicrobial evaluation; 2018. doi: 10.7275/12222378.
42. Al Ostoot FH, Zabiulla SS, Salah SA, Khanum SA. Recent investigations into synthesis and pharmacological activities of phenoxy acetamide and its derivatives (chalcone, indole and quinoline) as possible therapeutic candidates. J Iran Chem Soc. 2021;18(8):1839-75. doi: 10.1007/s13738-021-02172-5.
43. Yadav CS. Recent advances in the synthesis of pyrazoline derivatives from chalcones as potent pharmacological agents: a comprehensive review. Results Chem. 2024 Jan;7:101326. doi: 10.1016/j.rechem.2024.101326.
44. Ohikhena FU, Wintola OA, Afolayan AJ. Evaluation of the antibacterial and antifungal properties of phragmanthera capitata (Sprengel) balle (Loranthaceae) a mistletoe growing on rubber tree using the dilution techniques. ScientificWorldJournal. 2017;2017(1):9658598. doi: 10.1155/2017/9658598, PMID 28642934.
45. Khan Y, Khan S, Hussain R, Maalik A, Rehman W, Attwa MW. The synthesis *in vitro* bio-evaluation and in silico molecular docking studies of pyrazoline thiazole hybrid analogues as promising anti-α-glucosidase and anti-urease agents. Pharmaceuticals (Basel). 2023;16(12):1650. doi: 10.3390/ph16121650, PMID 38139777.
46. Sharma H, Chawla PA, Bhatia R. 1,3,5-pyrazoline derivatives in cns disorders: synthesis biological evaluation and structural insights through molecular docking. CNS Neurol Disord Drug Targets. 2020;19(6):448-65. doi: 10.2174/1871527319999200818182249, PMID 32811418.
47. Yousif OA, Mahdi MF, Raauf AM. Design synthesis preliminary pharmacological evaluation molecular docking and ADME studies of some new pyrazoline isoxazoline and pyrimidine derivatives bearing nabumetone moiety targeting cyclooxygenase enzyme. J Contemp Med Sci. 2019;5(1):41-50. doi: 10.22317/jcms.v5i1.521.